

Supplementary Information

Characterization of the Flavoenzyme XiaK as an *N*-Hydroxylase and Implications in Indolosesquiterpene Diversification[†]

Qingbo Zhang,^{‡a} Huixian Li,^{‡ab} Lu Yu,^c Yu Sun,^d Yiguang Zhu,^a Hanning Zhu,^a Liping Zhang,^a Shu-Ming Li,^e Yuemao Shen,^f Changlin Tian,^c Ang Li,^d Hung-wen Liu,^{g*} and Changsheng Zhang^{a*}

^aCAS Key Laboratory of Tropical Marine Bio-resources and Ecology, RNAM Center for Marine Microbiology, Guangdong Key Laboratory of Marine Materia Medica, South China Sea Institute of Oceanology, Chinese Academy of Sciences, 164 West Xingang Road, Guangzhou 510301, China;

^bInstitute of Marine Natural Products, School of Marine Sciences, Sun Yat-sen University, Guangzhou, 135 West Xingang Road, Guangzhou 510006, China;

^cHefei National Laboratory of Microscale Physical Sciences, School of Life Science, University of Science and Technology of China, Hefei, 230027, China, and High Magnetic Field Laboratory, Chinese Academy of Sciences, Hefei, 230031, P. R. China;

^dState Key Laboratory of Bioorganic and Natural Products Chemistry, Shanghai Institute of Organic Chemistry, Chinese Academy of Sciences, 345 Lingling Road, Shanghai 200032, China;

^eInstitut für Pharmazeutische Biologie und Biotechnologie, Philipps-Universität Marburg, Deutschhausstrasse 17a, 35037 Marburg, Germany;

^fState Key Laboratory of Microbial Technology, School of Life Science, Shandong University, Jinan 250100, China;

^gDivision of Chemical Biology and Medicinal Chemistry, College of Pharmacy and Department of Chemistry, University of Texas at Austin, Austin, TX, 78712, USA.

‡ Q. Zhang and H. Li contributed equally to this work.

Correspondence and requests for materials should be addressed to C.Z. (email: cchang2006@gmail.com) or H.w.L. (h.w.liu@mail.utexas.edu)

Contents

Author contributions	S3
Table S1 Strains, plasmids and primers used and generated in this study	S4
Table S2 The ^1H NMR data of compounds 13 , 17–19	S5
Table S3 The ^{13}C NMR data of compounds 13 , 17–19	S6
Table S4 Comparison of the kinetic parameters of XiaK and other <i>N</i> -oxidases	S7
Fig. S1 SDS-PAGE analysis of purified recombinant XiaK and the determination of FAD as the non-covalent binding cofactor in XiaK	S8
Fig. S2 UV-Vis spectral and LC-MS analysis of XiaK reaction products with XMA (1)	S9
Fig. S3 The spectral data of 13	S10
Fig. S4 The EPR experiment data of XMA (1) and OXM (7)	S17
Fig. S5 ^{15}N -labelling related studies	S18
Fig. S6 Construction of the in-frame deletion mutant XM47i (ΔxiaPi)	S22
Fig. S7 Comparison of theoretical simulation and experimental EPR spectra of ^{14}N - 12 and ^{15}N - 12	S23
Fig. S8 Estimation of the spin concentration of 12	S23
Fig. S9 Phylogenetic analysis of XiaK with other flavoenzymes	S24
Fig. S10 Comparison of well aligned XiaK structure model and the crystal structures of class A flavoprotein monooxygenases	S25
Fig. S11 Sequence comparison of XiaK and four class A flavoprotein monooxygenases ..	S26
Fig. S12 UV-Vis and HRESIMS spectra of 16	S27
Fig. S13 Comparison of UV-vis spectra of 1 , 17 and 18	S28
Fig. S14 The spectral data of 17	S29
Fig. S15 The spectral data of 18	S36
Fig. S16 The Spectral data of 19	S43
Fig. S17 Stability of compounds 12 stored in organic solvents	S51
Fig. S18 The hypothesized mechanism for the formation of DXMs A-C (8–10)	S52
Supplementary Reference	S53

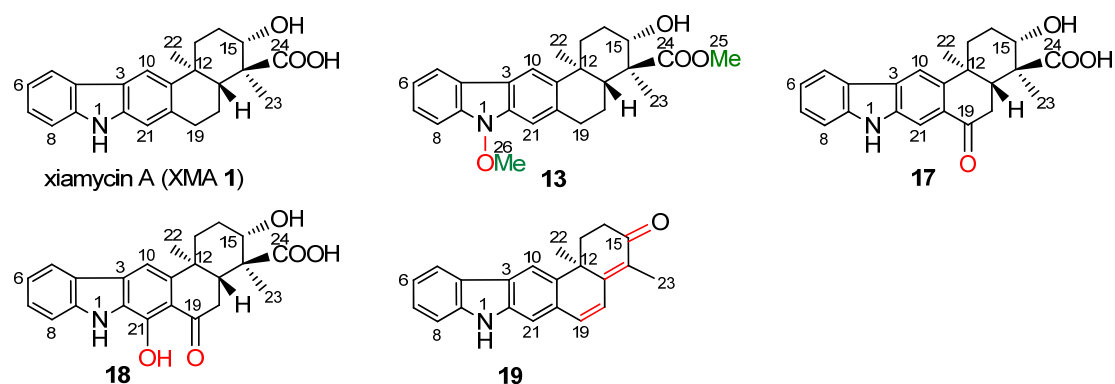
Author Contributions

Q.Z., H.L. and C.Z. conceived and designed the study. Q.Z., Y.S and A.L. performed chemical studies. H.L., Y.Z. and H.Z. performed molecular and biochemical experiments. L.Y. and C.T. performed EPR experiments, L.Z. performed bioinformatics analysis. S.-M.L, Y.-M.S., A.L., H.w.L. and C.Z. analyzed and discussed the results. Q.Z., H.L., L.Y., H.w.L. and C.Z. prepared the manuscript.

Table S1 Strains, plasmids and primers used and generated in this study.

Strains/Plasmids	Characteristic(s)	Sources
<i>E.coli</i>		
DH5α	Host strain for cloning	Invitrogen
ET12567	Donor strain for conjugation	1
BL21(DE3)	Host strain for protein expression	Novagen
<i>Streptomyces</i> sp.		
<i>S. coelicolor</i> YF11	Host strain for gene cluster and protein expression	2
<i>S. pactum</i> SCSIO 02999	Wild type, xiamycin/oxiamycin producer	3
XM47i	<i>XiaP</i> gene in-frame deletion mutant of SCSIO 02999	This work
Plasmids		
BT340	Cm ^r , express FLP-recombinase to form in-frame deletion genes	4
pUZ8002	Km ^r , including <i>tra</i> for conjugation	5
pSET152	Ap ^r , integrative vector for <i>Streptomyces</i> heterologous expression	6
pPWW50A	Ap ^r , <i>amp</i> in pPWW50 was replaced by <i>aac(3)IV</i> and <i>oriT</i>	7
pET28a	Km ^r	Novagen
pCSG2407	cosmid carrying the intact <i>xia</i> gene cluster	3
pCSG2517	A pCSG2407 derivative where <i>xiaP</i> was disrupted by <i>aac(3)IV</i>	3
pCSG2547	A pCSG2517 derivative where <i>xiaP</i> was in-frame deleted	This work
pCSG2562	A pCSG2557 derivative where <i>neo</i> was disrupted by <i>aac(3)IV</i>	This work
pCSG2671	about 30 kb <i>EcoR</i> I fragment containing the <i>xia</i> gene cluster from pCSG2407 inserted into pSET152 digested with <i>EcoRI</i>	This work
pCSG2607	1.8 kb <i>xiaK</i> PCR fragment (<i>NdeI/BglII</i>) from SCSIO 02999 inserted into pET28a for <i>E.coli</i> expression inserted into pET28a (<i>NdeI/BamHI</i>)	This work
pCSG2701	1.8 kb <i>xiaK</i> PCR fragment (<i>NdeI/BglII</i>) from SCSIO 02999 inserted into pPWW50A(<i>NdeI/BamHI</i>)	This work
Primers		
	Target gene	Sequence
For diagnostic PCR		
XiaP-1F	<i>xiaP</i>	5'- GCGAACTGGCAGCGATTGTG -3'
XiaP-1R		5'- GC GGATCTGGTAGGCGATGC -3'
orf1-1F	<i>orf1</i>	5'- GTACTGCGTGAAGCCCGACC -3'
orf1-1R		5'- CCCAGAACTCGGCCGGTGTAC -3'
For gene cloning		
XiaK-3F	<i>xiaK</i>	5'-GGAAGACATATGTTGGACGTAGAAGTGCC-3', <i>NdeI</i>
XiaK-3R		5'- CAACATAGATCTCAGGAAGGTGTGG -3', <i>Bgl II</i>

Table S2 The ^1H NMR data of compounds **13**, **17–19**.



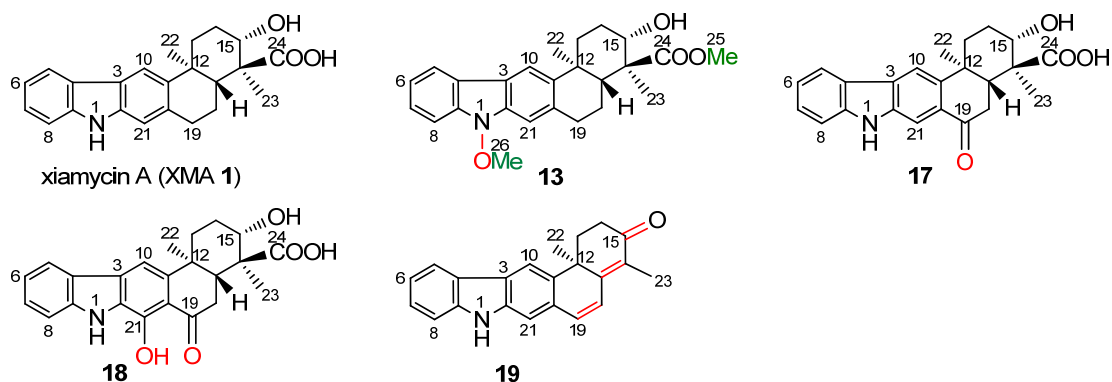
No.	1^a	13^b	17^c	18^c	19^c
	δ_{H} (mult, <i>J</i> in Hz)	δ_{H} (mult, <i>J</i> in Hz)			
NH	10.9 (s) ^c				
5	7.98 (d, 8.0)	8.09 (d, 8.0)	8.16 (d, 8.0)	8.07 (d, 7.8)	8.07 (d, 7.8)
6	7.10 (ddd, 8.0, 7.0, 1.0)	7.20 (ddd, 8.0, 7.0, 1.0)	7.20 (m)	7.18 (dd, 7.8, 7.2)	7.15 (ddd, 8.4, 7.2, 1.2)
7	7.30 (ddd, 8.0, 7.0, 1.0)	7.40 (ddd, 8.0, 7.0, 1.0)	7.47 (m)	7.44 (dd, 7.8, 7.2)	7.36 (ddd, 8.4, 7.2, 1.2)
8	7.36 (d, 8.0)	7.49 (d, 8.0)	7.47 (m)	7.50 (d, 8.4)	7.43 (d, 7.8)
10	7.93 (s)	8.05 (s)	8.12 (s)	7.55 (s)	8.16 (s)
13	2.60 (td, 13.0, 3.0); 1.79 (m)	2.54 (m); 1.59 (m)	2.73 (m); 1.94 (m)	2.62 (m); 1.93 (m)	2.98 (m); 2.35 (m)
14	1.90 (m)	1.75 (m)	1.96 (m)	1.93 (m)	2.85 (m); 2.67 (m)
15	4.11 (dd, 9.0, 7.5)	3.88 (m)	4.13 (m)	4.10 (m)	
15-OH	4.71 (m)	4.80 (d, 5.0)			
17	2.21 (dd, 12.5, 2.0)	1.99 (m)	2.67 (m)	2.58 (m)	
18	2.00 (m); 1.56 (m)	1.93 (m); 1.26 (m)	2.96 (m); 2.43 (d, 17.5)	3.01 (dd, 12, 14.5); 2.39 (dd, 12, 14.5)	6.76 (d, 9.6)
19	3.09 (m)	3.09 (m); 2.96 (m)			7.05 (d, 9.6)
21	7.07 (s)	7.17 (s)	8.06 (s)		7.35 (s)
22	1.30 (s)	1.21 (s)	1.39 (s)	1.32 (s)	1.49 (s)
23	1.26 (s)	1.14 (s)	1.33 (s)	1.30 (s)	1.92 (s)
24-OH	12.1 (s) ^c				
25		3.62 (s)			
26		4.04 (s)			

^a 500 MHz for ^1H NMR CD_3OD , tetramethylsilane (TMS) as an internal standard;

^b 500MHz for ^1H NMR and $\text{DMSO}-d_6$, TMS as an internal standard;

^c 600 MHz for ^1H NMR CD_3OD , TMS as an internal standard.

Table S3 The ^{13}C NMR data of compounds **13**, **17–19**.



No.	1^a	13^b	17^c	18^c	19^c
2	138.1 C	136.2 C	139.6 C	128.1 C	139.5 C
3	121.1 C	118.2 C	129.5 C	130.8 C	125.8 C
4	122.6 C	119.9 C	123.8 C	124.2 C	124.4 C
5	118.7 CH	120.4 CH	122.2 CH	122.2 CH	121.2 CH
6	117.5 CH	120.0 CH	120.3 CH	120.5 CH	120.2 CH
7	124.2 CH	125.9 CH	128.6 CH	128.6 CH	127.2 CH
8	109.7 CH	108.5 CH	112.2 CH	112.8 CH	112.0 CH
9	140.0 C	138.0 C	143.9 C	143.3 C	142.6 C
10	114.5 CH	116.4 CH	116.1 CH	106.7 CH	116.7 CH
11	139.9 C	142.2 C	147.5 C	147.4 C	138.0 C
12	36.4 C	36.8 C	38.2 C	38.7 C	40.7 C
13	37.0 CH ₂	37.2 CH ₂	38.2 CH ₂	38.2 CH ₂	35.0 CH ₂
14	26.6 CH ₂	27.4 CH ₂	28.3 CH ₂	28.3 CH ₂	35.2 CH ₂
15	74.4 CH	73.9 CH	76.8 CH	76.2 CH	200.7 C
16	53.0 C	53.5 C	54.3 C	54.3 C	129.4 C
17	45.7 CH	46.0 CH	46.8 CH	46.6 CH	160.2 C
18	20.7 CH ₂	20.8 CH	38.7 CH ₂	38.6 CH ₂	123.6 CH
19	30.1 CH ₂	30.2 CH ₂	201.3 C	206.9 C	136.7 CH
20	132.3 C	133.7 C	130.2 C	112.4 C	130.3 C
21	109.1 CH	107.7 CH	110.7 CH	152.2 C	112.0 CH
22	24.7 CH ₃	25.4 CH ₃	24.8 CH ₃	24.9 CH ₃	31.4 CH ₃
23	9.7 CH ₃	10.9 CH ₃	11.21 CH ₃	11.5 CH ₃	10.7 CH ₃
24	180 C	177.3 C	180 C	181.3 C	
25		51.8 CH ₃			
26		63.4 CH ₃			

^a 125 MHz for ^{13}C NMR, CD₃OD, tetramethylsilane (TMS) as an internal standard;

^b 150 MHz for ^{13}C NMR, DMSO-*d*₆ and TMS as an internal standard;

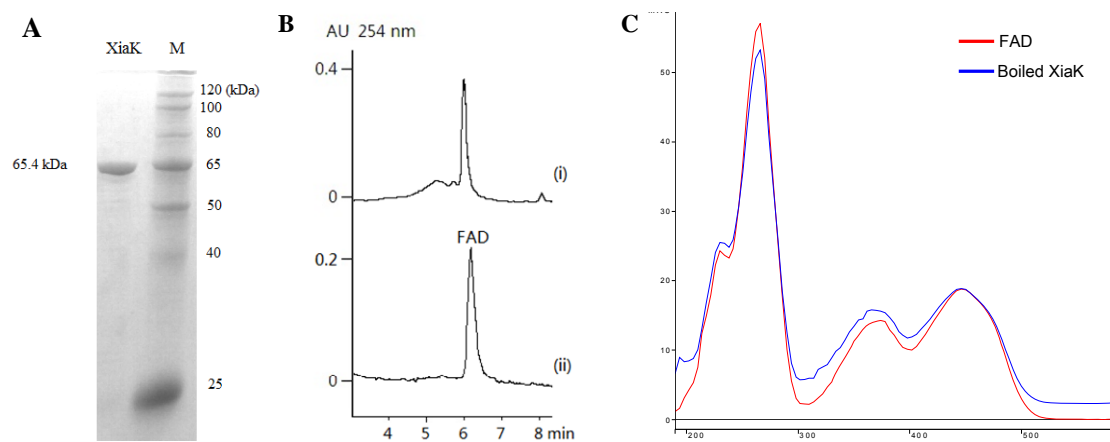
^c 150 MHz ^{13}C NMR, CD₃OD and TMS as an internal standard.

Table S4 Comparison of the kinetic parameters of XiaK and other *N*-oxidases.

Enzyme	Substrate	K_m [μM]	k_{cat} [min ⁻¹]	k_{cat}/K_m [μM ⁻¹ min ⁻¹]
XiaK		16.2 ± 3.3	260.4 ± 14.1	16.1
PvdA ⁸		600 ± 70	24 ± 3	0.04
SidA ⁹		490 ± 70	102 ± 6	0.21
NbtG ¹⁰		350 ± 50	18.6 ± 1.2	0.053
CreE ¹¹		124.8 ± 5.0	68.4 ± 0.5	0.55
FzmM ¹²		790 ± 70	148.8 ± 0.4	0.19
PrnD ¹³		379 ± 34	6.5 ± 0.62	0.017
CalE10 ¹⁴		7.6 ± 1.2	0.04 ± 0.01	0.0053
AurF ¹⁵		5.24 ± 0.64	6.21 ± 0.52	1.21

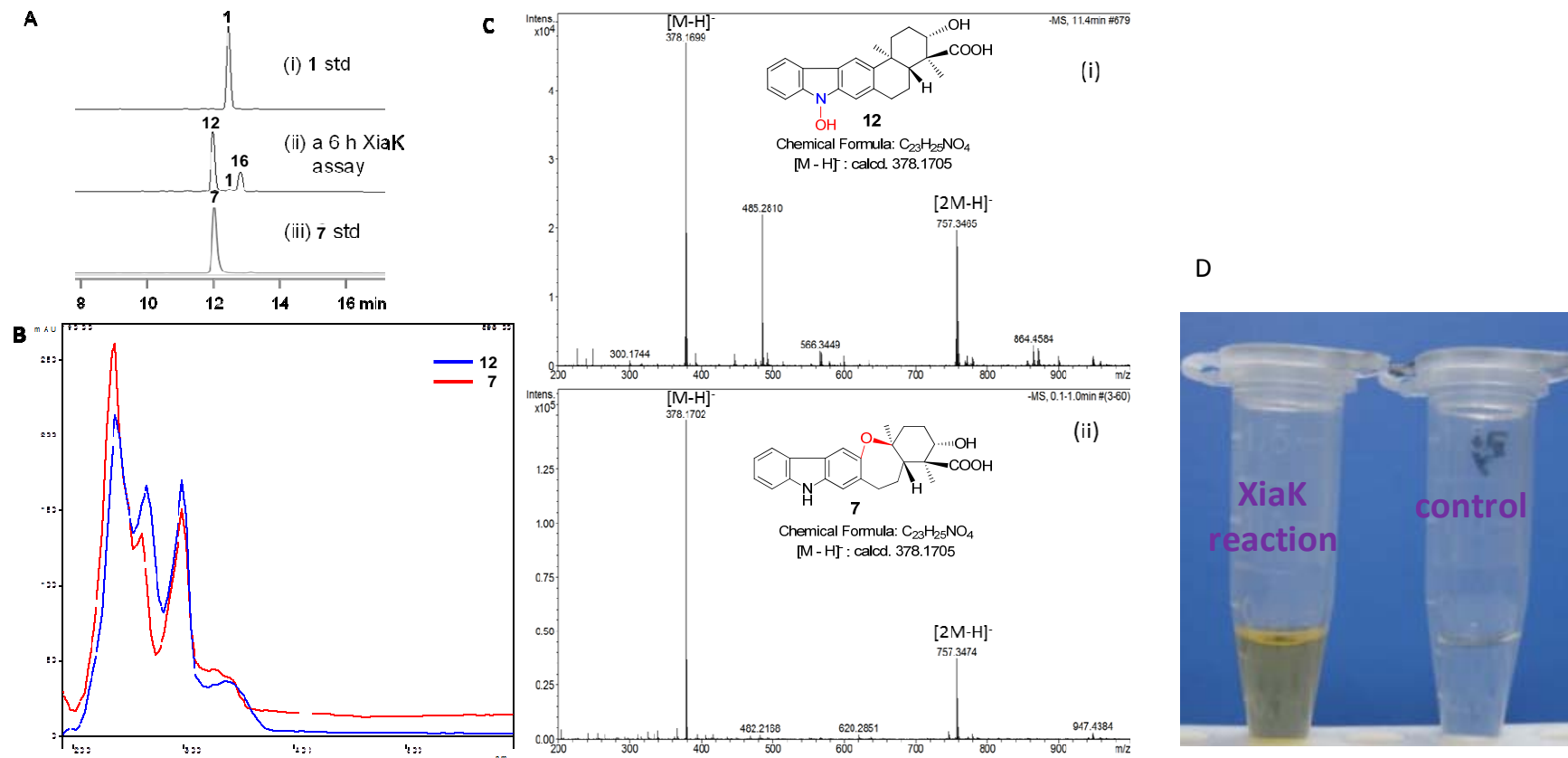
Note: PvdA, SidA, NbtG, CreE and FzmM are flavoenzymes, while PrnD, CalE10 and AurF are P450 enzymes. Shown in the table (except XiaK) are the kinetic parameters for an *N*-hydroxylation reaction to convert a primary amine to a hydroxylamine.

Fig. S1 SDS-PAGE analysis of purified recombinant XiaK and the determination of FAD as the non-covalent binding cofactor in XiaK.



(A) SDS-PAGE analysis of XiaK. The expected size of N-His₆-tagged XiaK (65.4 kDa) was indicated. Lane M, protein molecular weight standards (ProteinRulerTM III, TransGen Biotech). (B) HPLC analysis of boiled XiaK. (i) boiled XiaK; (ii) FAD standard. (C) Comparison of UV-Vis spectra of the supernatants of boiled XiaK and the FAD standard.

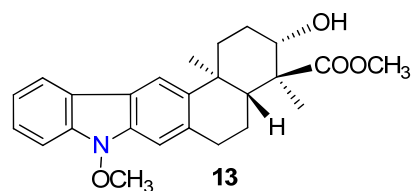
Fig. S2 UV-Vis spectral and LC-MS analysis of XiaK reaction products with XMA (**1**).



(A) HPLC analysis of XiaK-catalyzed reaction. (i) XMA (**1**) standard; (ii) a XiaK assay comprising of 300 μ M XMA (**1**), 1 mM NADPH, and 5 μ M XiaK in 50 mM Na₂HPO₄-NaH₂PO₄ buffer (pH 8.0) for 6 h at 30 °C; (iii) OXM (**7**) standard. (B) The UV-vis spectral comparison of NOXM (**12**) and OXM (**7**). (C): LC-HRESIMS spectra of **12** (i) and **7** (ii); (D) The yellow color of a typical XiaK reaction with **1** for 2 h versus a control lacking XiaK.

Fig. S3 The spectral data of **13**. (500 MHz for ^1H NMR, 125 MHz for ^{13}C NMR, DMSO- d_6)

(A) The HRESIMS spectrum of **13**



Chemical Formula: $\text{C}_{25}\text{H}_{29}\text{NO}_4$

$[\text{M} + \text{Na}]^+$: Calcd. 430.1989

$[\text{M} + \text{K}]^+$: Calcd. 446.1733

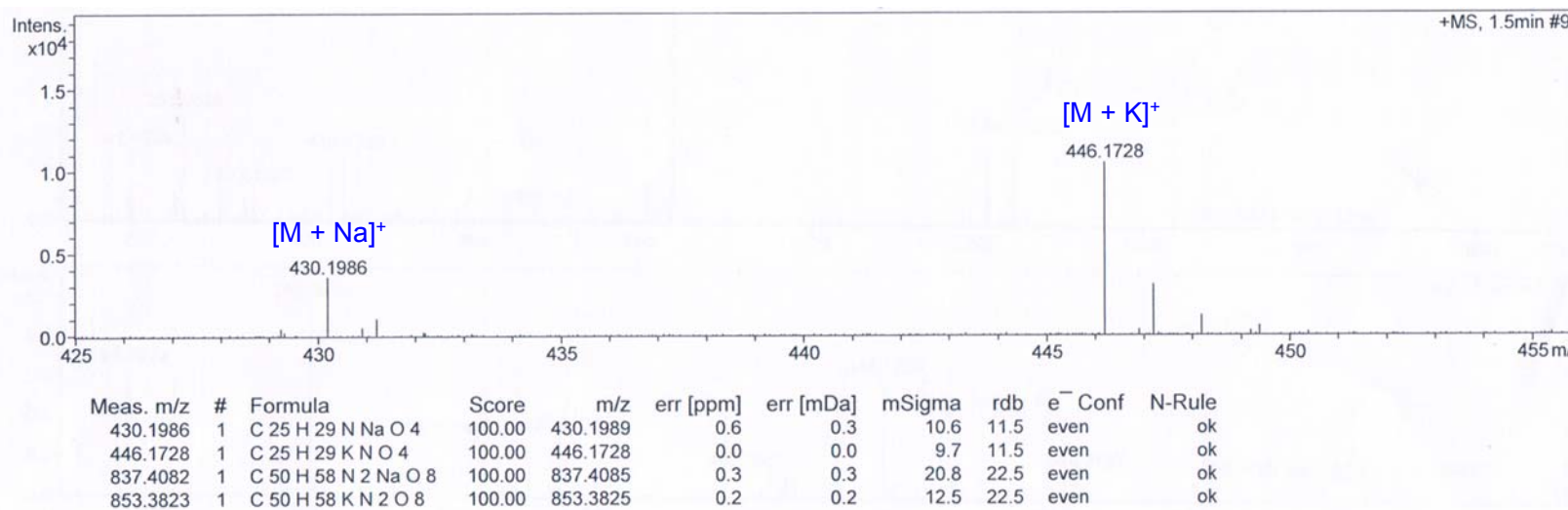


Fig. S3 The spectral data of **13**. (500 MHz for ^1H NMR, 125 MHz for ^{13}C NMR, DMSO- d_6)

(B) The ^1H -NMR spectrum of 13

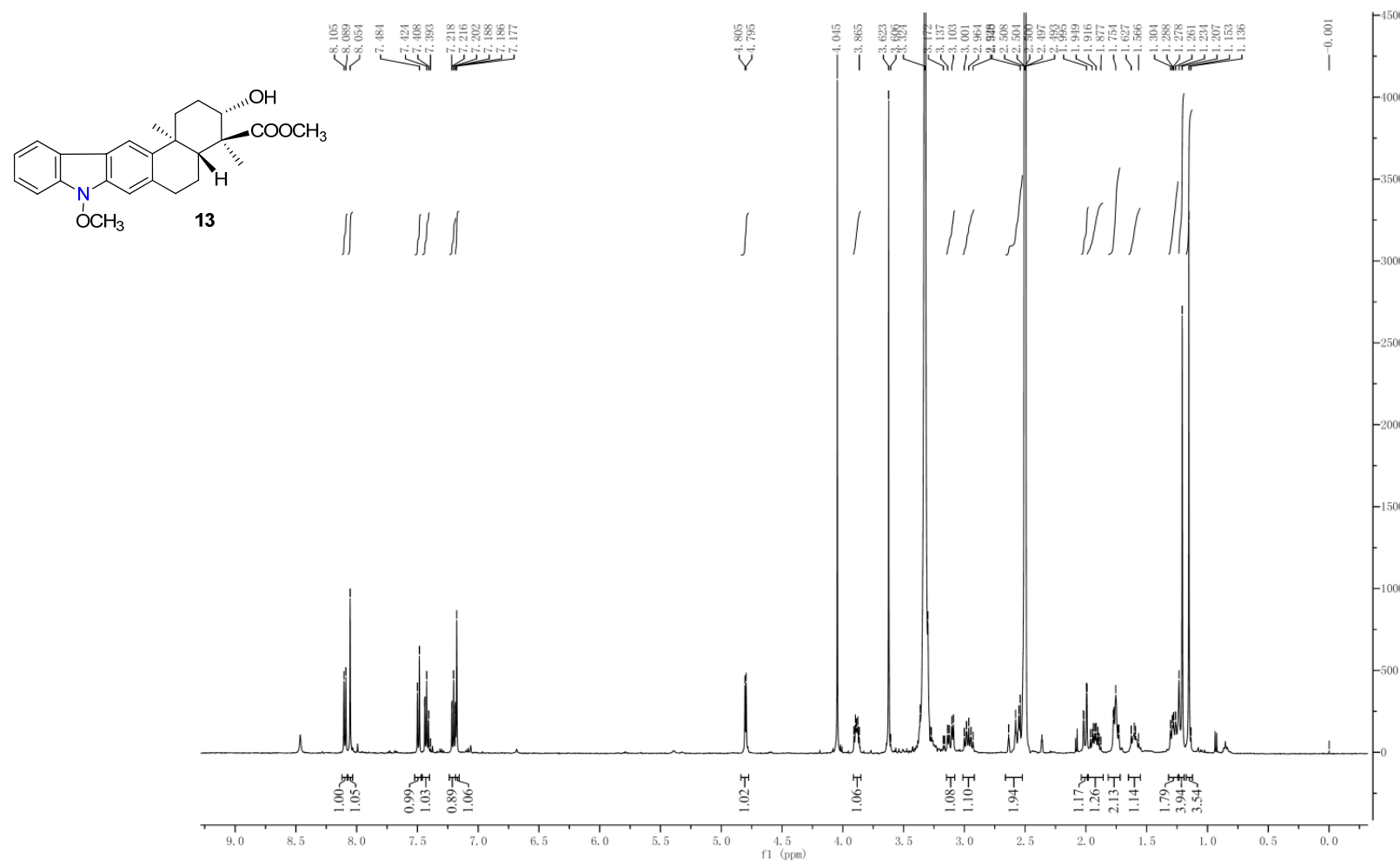


Fig. S3 The spectral data of **13**. (500 MHz for ^1H NMR, 125 MHz for ^{13}C NMR, DMSO- d_6)

(C) The ^{13}C -NMR spectrum of **13**

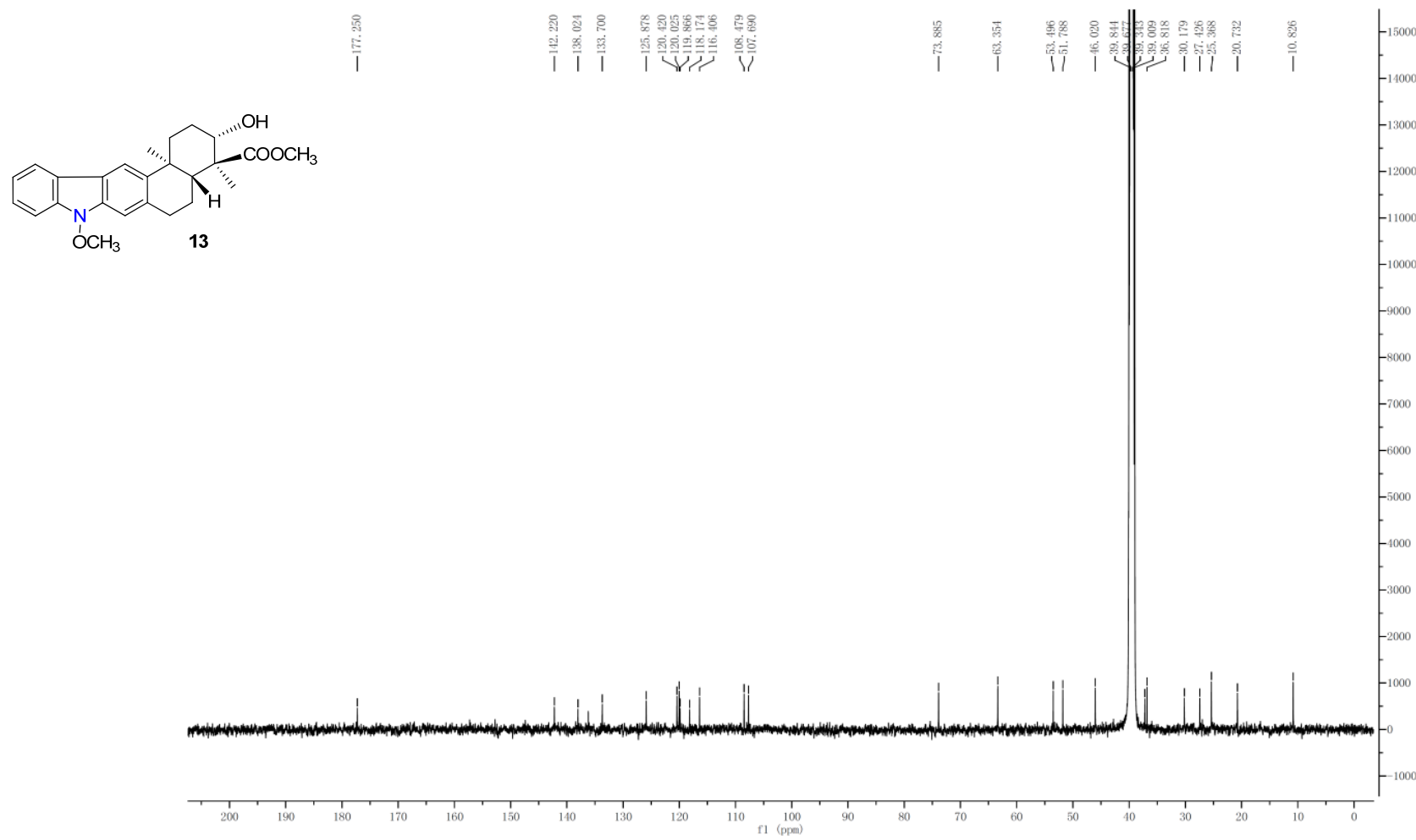


Fig. S3 The spectral data of **13**. (500 MHz for ^1H NMR, 125 MHz for ^{13}C NMR, DMSO- d_6)

(D) The DEPT135 spectrum of **13**

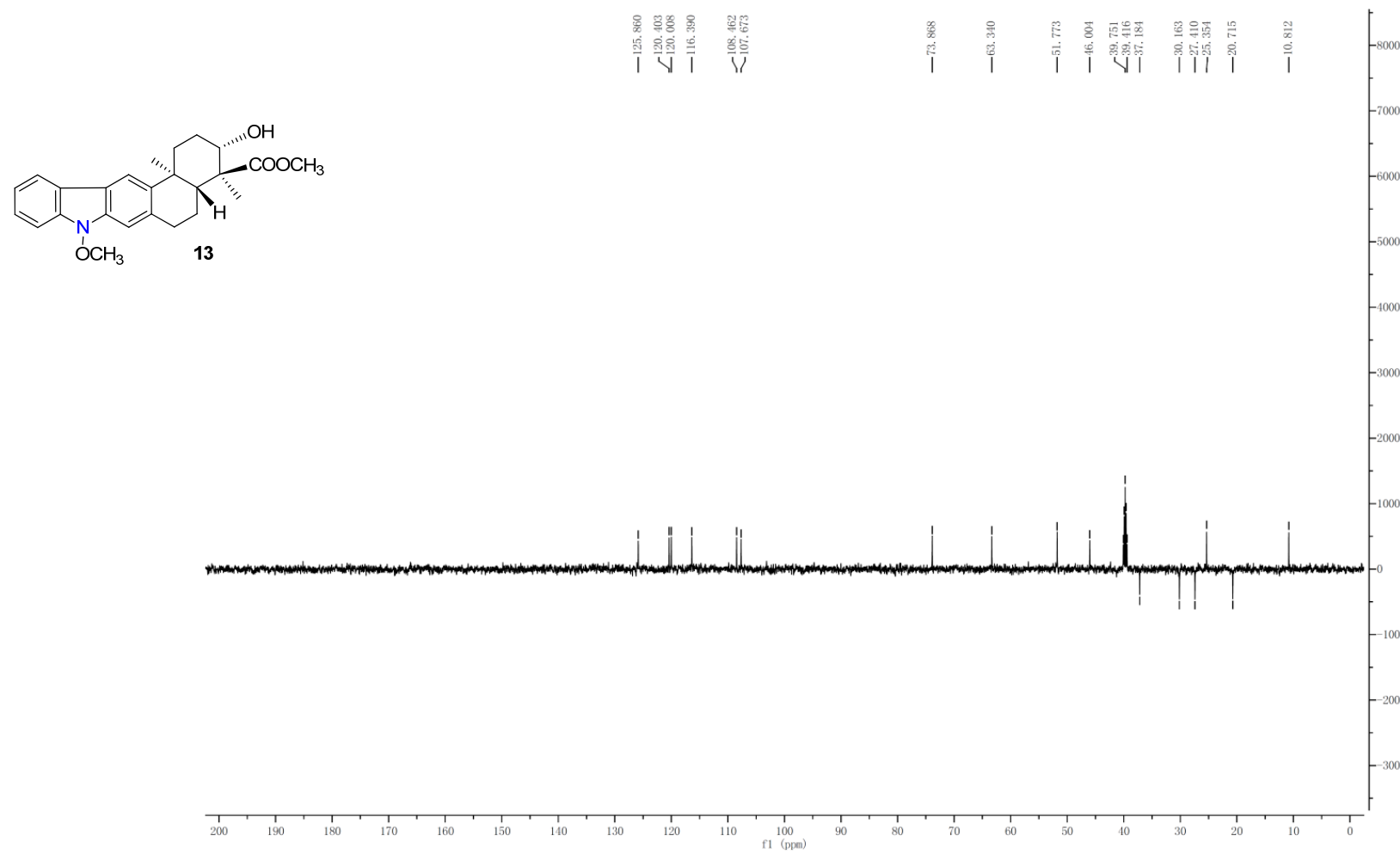


Fig. S3 The spectral data of **13**. (500 MHz for ^1H NMR, 125 MHz for ^{13}C NMR, DMSO- d_6)

(E) The HSQC spectrum of **13**

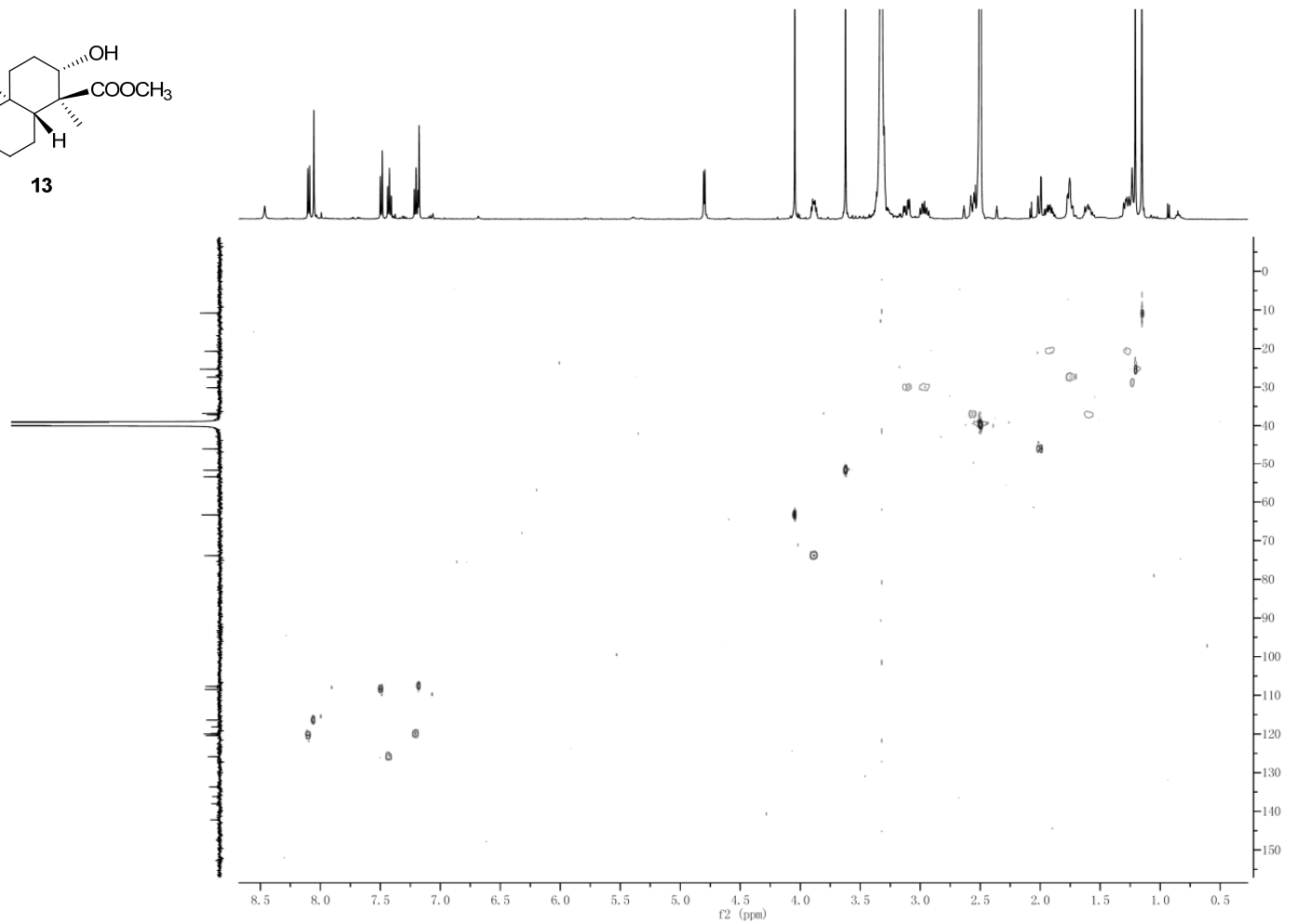
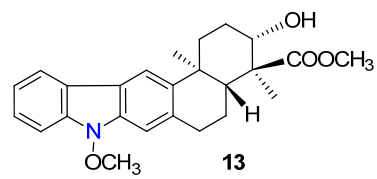


Fig. S3 The spectral data of **13**. (500 MHz for ^1H NMR, 125 MHz for ^{13}C NMR, DMSO- d_6)

(F) The ^1H - ^1H COSY spectrum of **13**

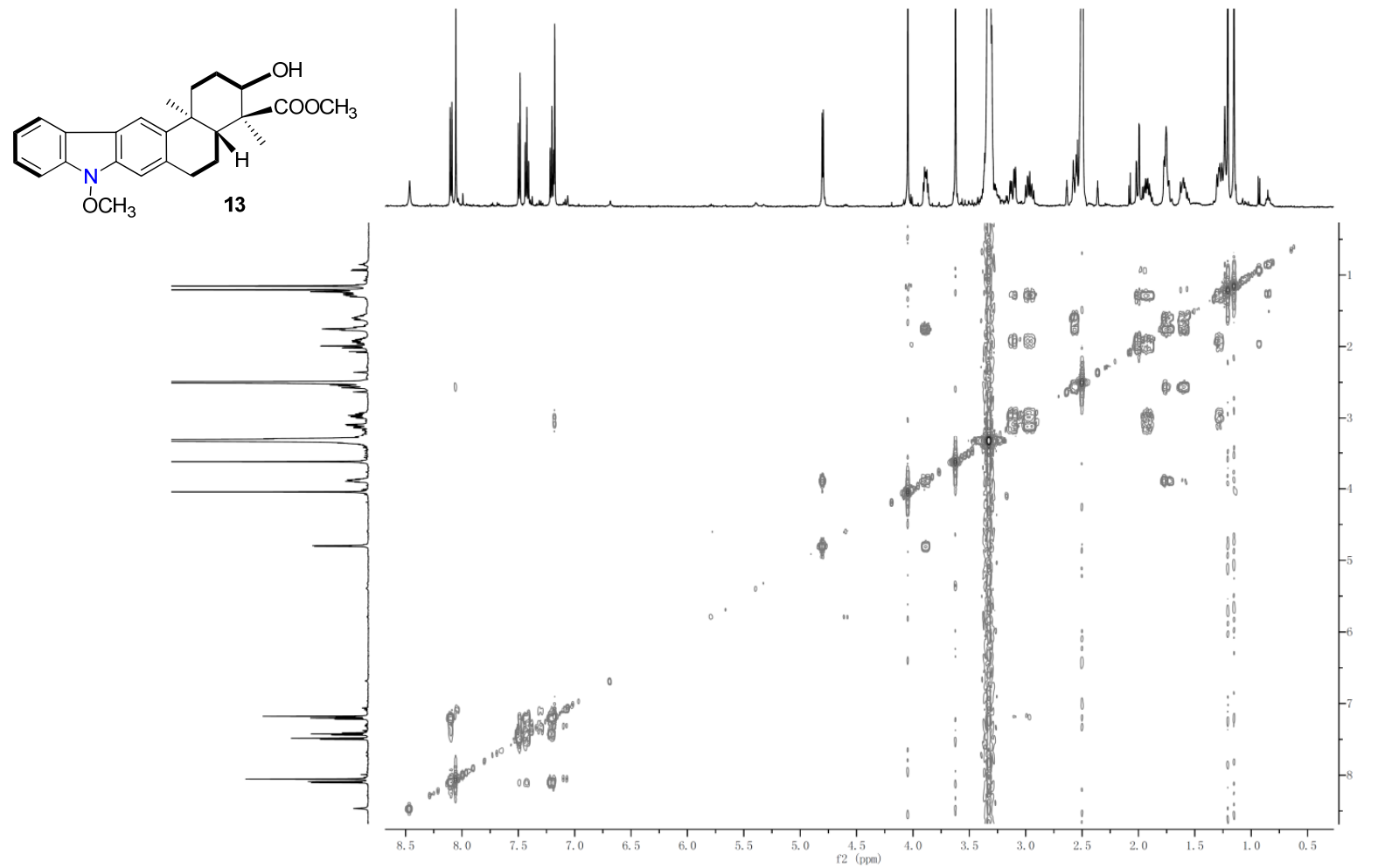


Fig. S3 The spectral data of **13**. (500 MHz for ^1H NMR, 125 MHz for ^{13}C NMR, DMSO- d_6)

(G) The HMBC spectrum of **13**

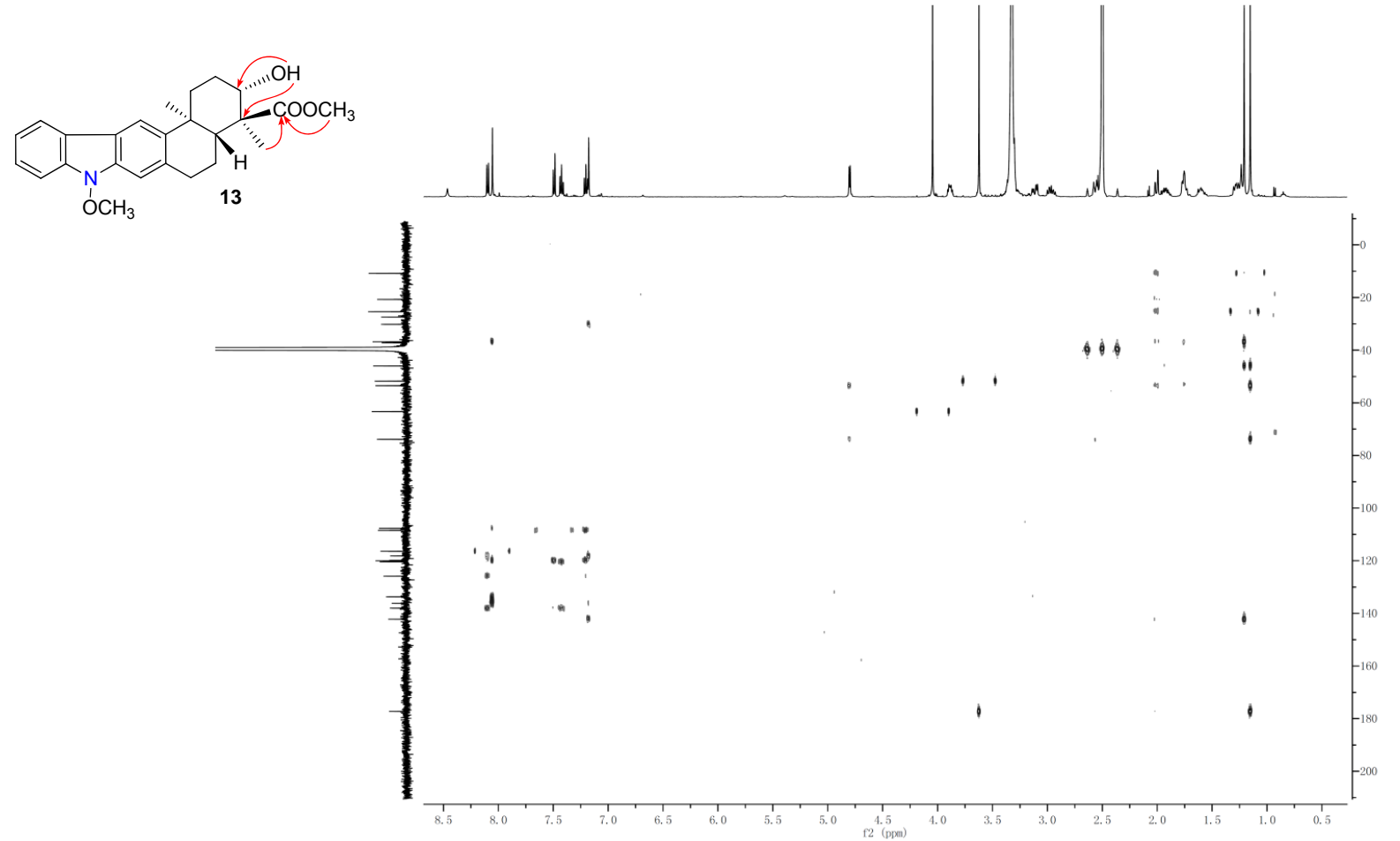
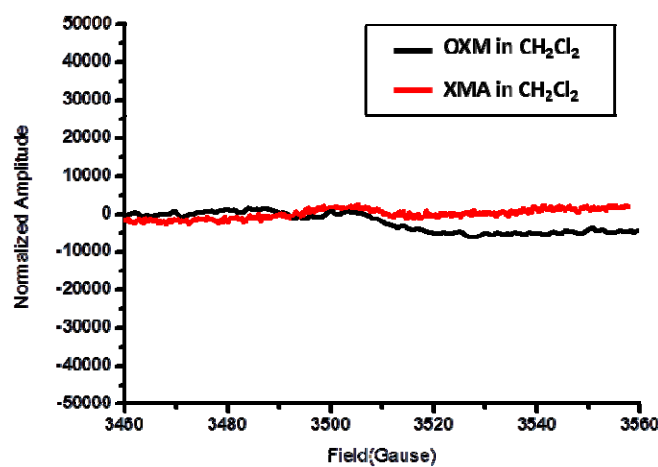


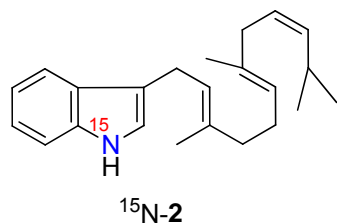
Fig. S4 The EPR spectra of XMA (**1**) and OXM (**7**)



The EPR data acquisition parameters for free radical analysis were as follows: Frequency, 9.390 GHz; Microwave power, 1 mW; Modulation Frequency, 100 kHz; Modulation Amplitude, 0.5 Gauss; Sweep Time, 40 s/scan; Different number of scans were accumulated for each sample until a reasonable S/N ratio was achieved.

Fig. S5 ^{15}N -labelling related studies.

(A) HRESIMS spectrum of chemically synthesized ^{15}N -labeled **2**.



Chemical Formula: $\text{C}_{23}\text{H}_{31}^{15}\text{N}$
[M + H] $^+$: Calcd. 323.2505

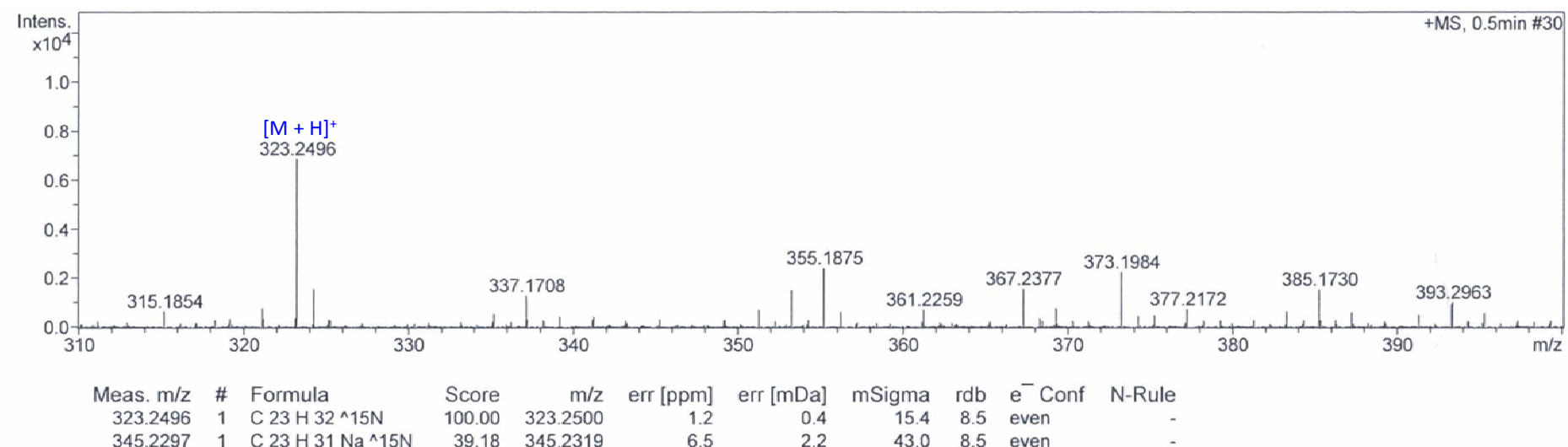


Fig. S5 ^{15}N -labelling related studies.

(B) ^1H NMR spectrum of chemically synthesized ^{15}N -labeled **2**. (500 MHz for ^1H NMR in CDCl_3)

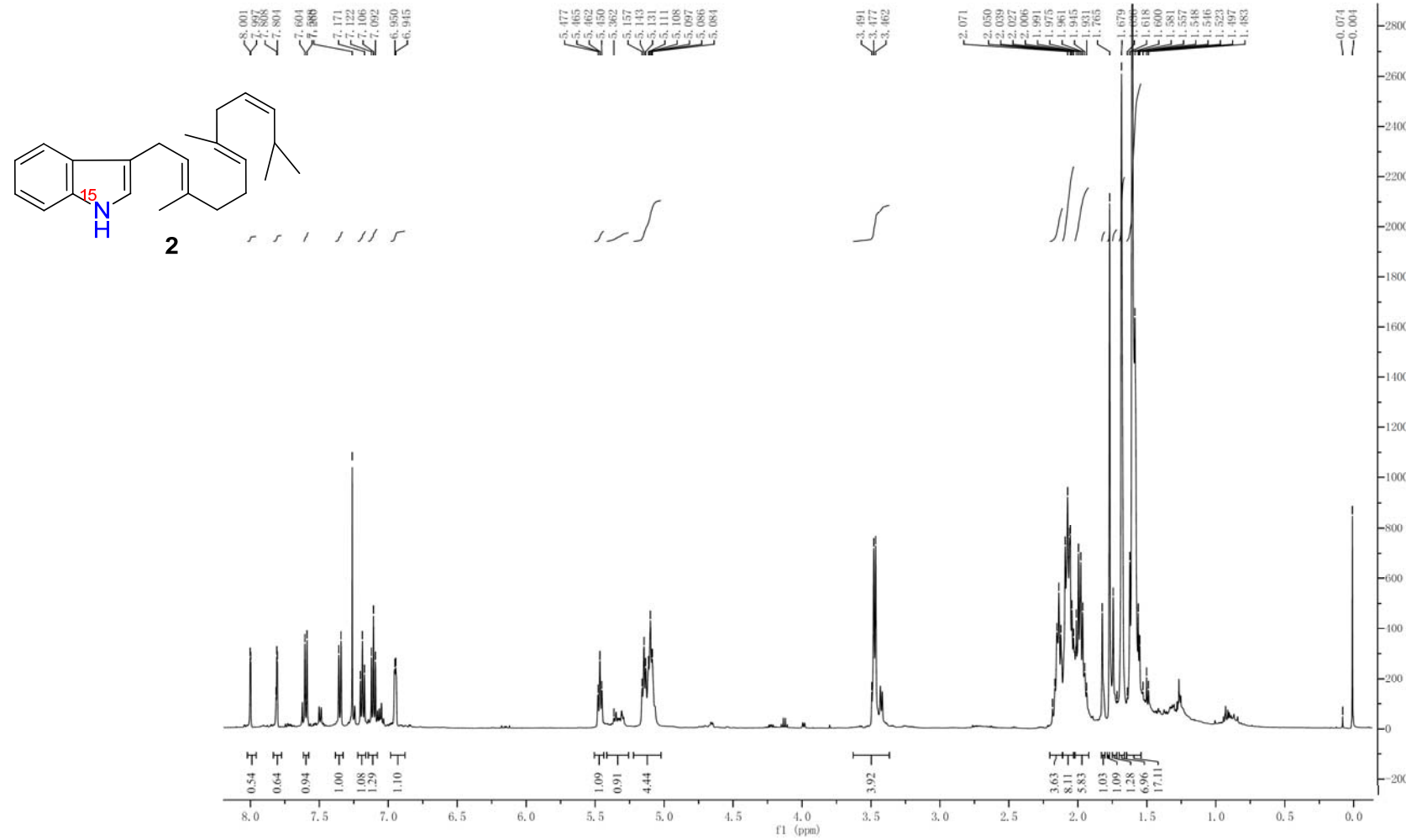


Fig. S5 ^{15}N -labelling related studies.

(C) HPLC analysis of feeding experiments of ^{15}N -labeled **2** in *S. pactum* XM47i. (i) feeding of ^{15}N -labeled **2** (147 mg) in *S. pactum* XM47i cultured in AM-4 meida (2 L); (ii) **2** standard; (iii) XMA (**1**) standard.

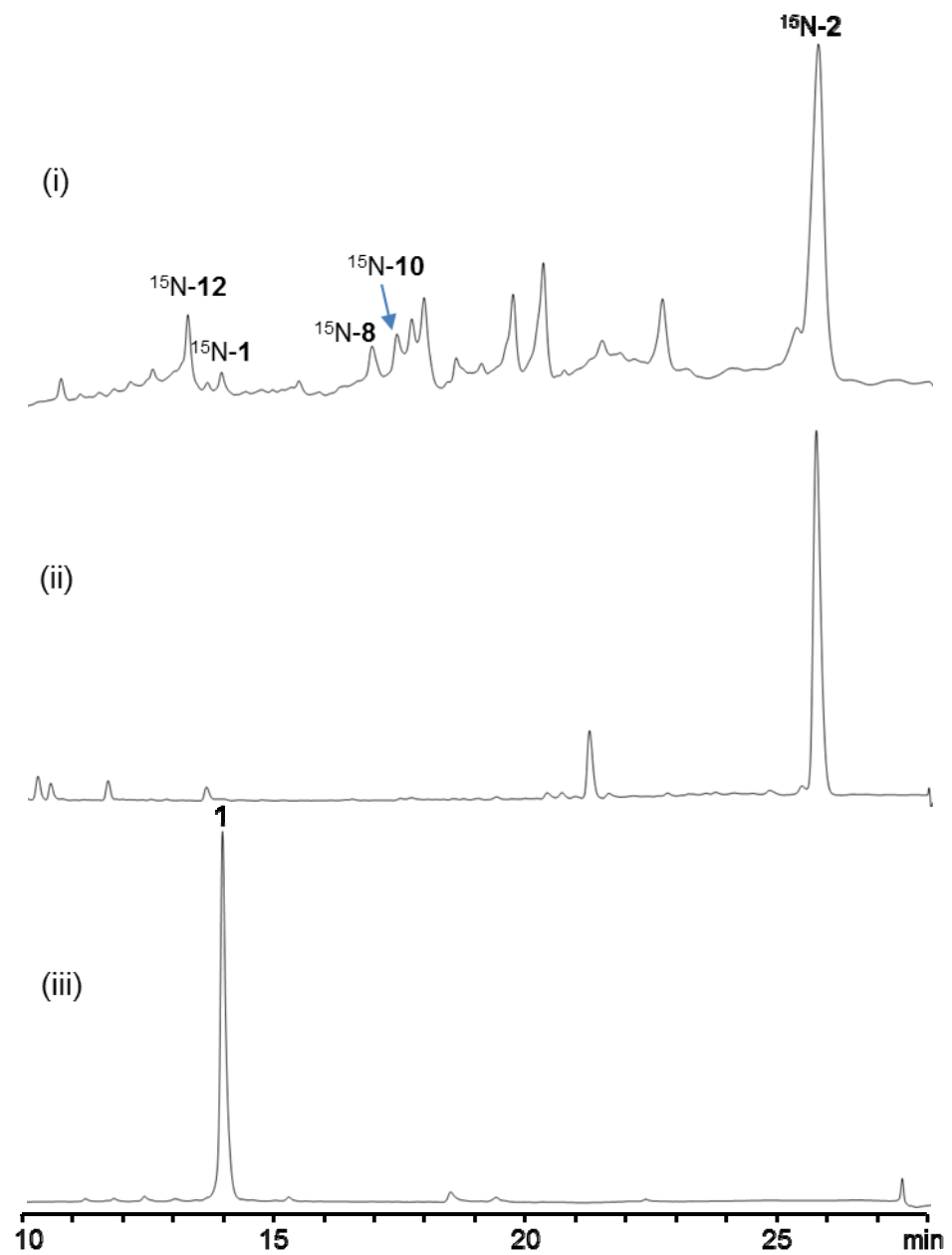


Fig. S5 ^{15}N -labelling related studies.

(D) HRESIMS of ^{15}N -labeled **1** isolated from *S. pactum* XM47i and ^{15}N -labeled **12** prepared from a XiaK reaction with ^{15}N -labeled **1**.

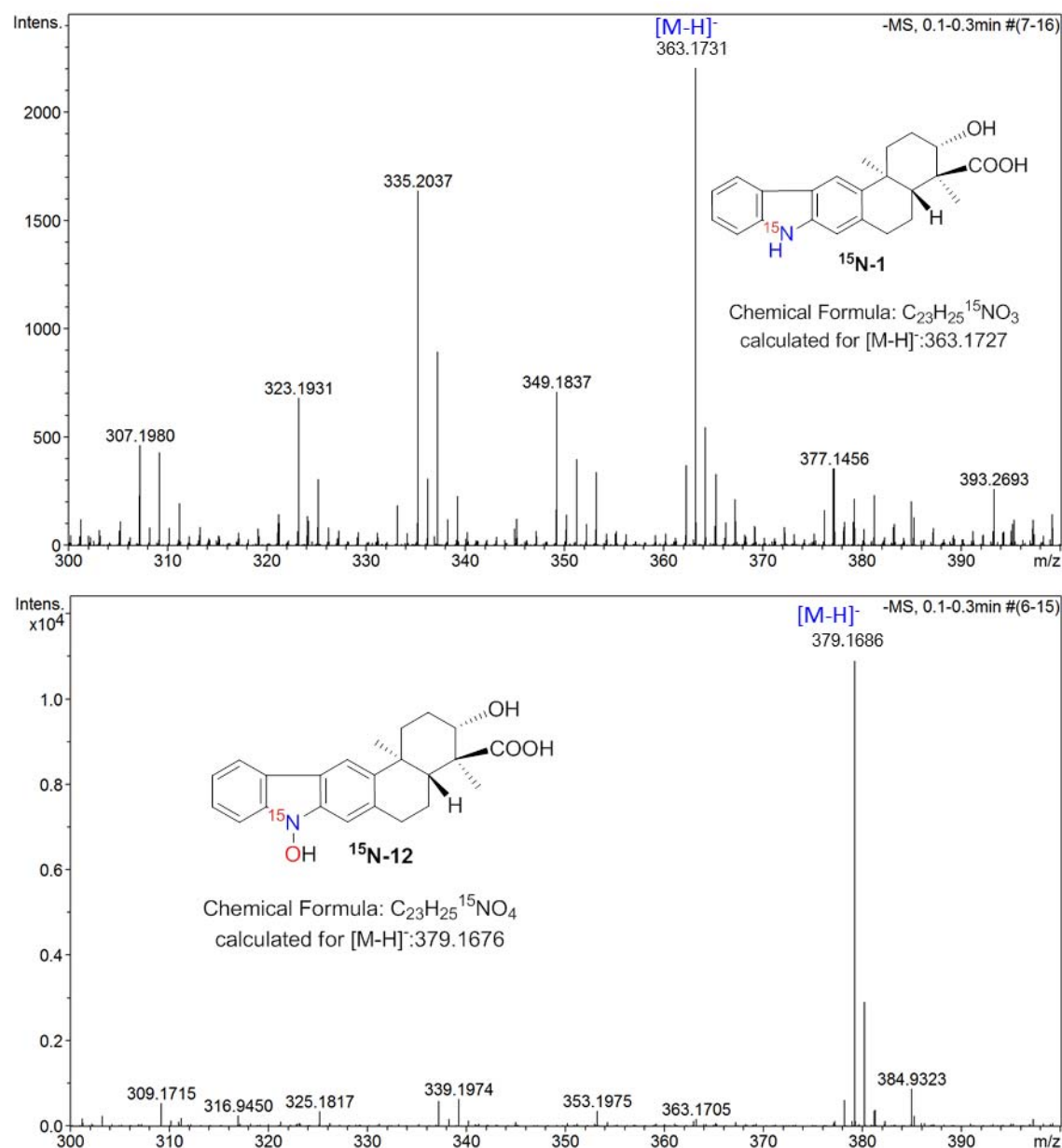
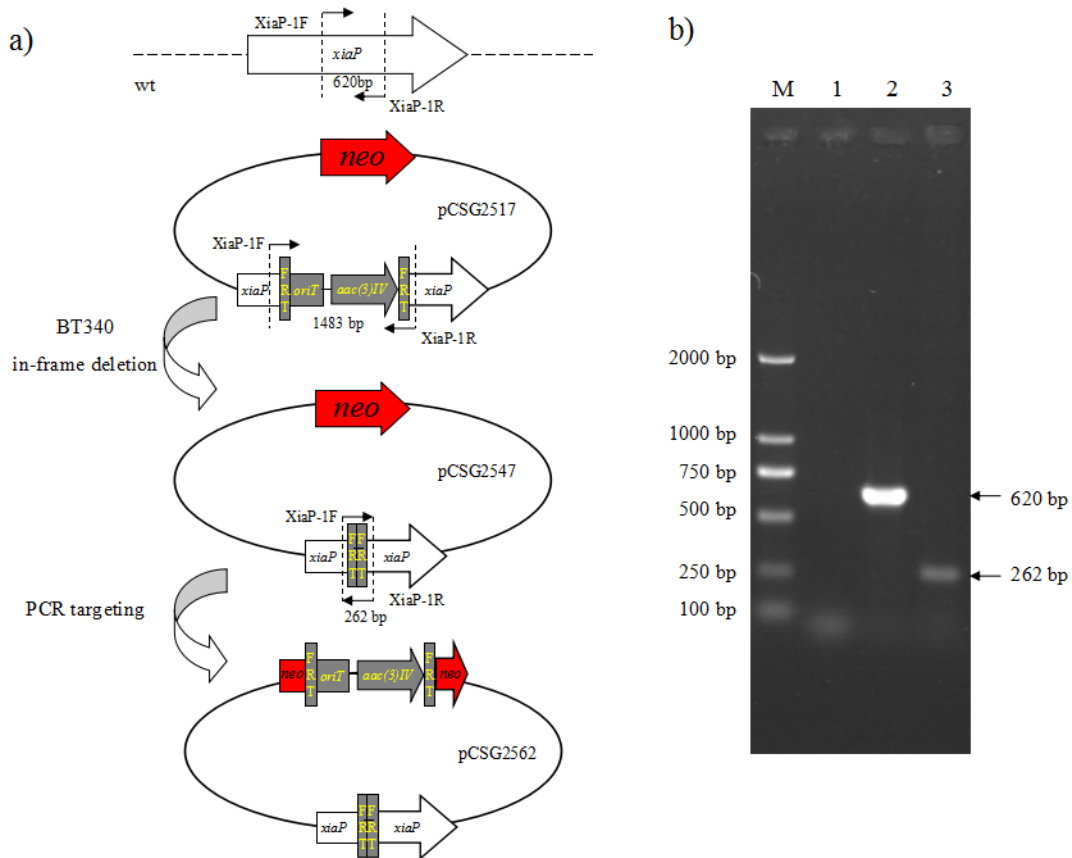


Fig. S6 Construction of the in-frame deletion mutant XM47i ($\Delta xiaP$).



The *xiaP* gene in-frame deletion mutations were individually confirmed by diagnostic PCR. (a) Construction of the *xiaP* in-frame deletion vector pCSG2562. Location of the diagnostic PCR primers XiaP-1F and XiaP-1R (Table S1) was indicated. Sizes of PCR products, 620 bp for the wild type strain *S. pactum* SCSIO 02999 and 262 bp for the mutant XM47i, were also indicated. (b) Gel electrophoresis of PCR products. DNA templates were from: DNA marker DL 2000 (Takara, lane M); ddH₂O (negative control, lane 1); wild type strain *S. pactum* SCSIO 02999 (lane 2) and mutant XM47i (lane 3).

Fig. S7 Comparison of theoretical simulation and experimental EPR spectra of ¹⁴N-12 and ¹⁵N-7.

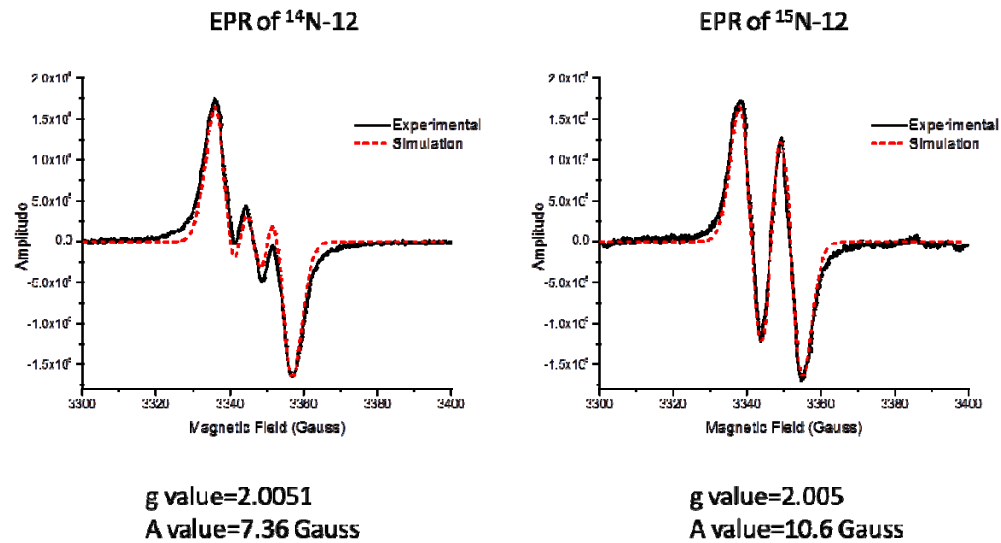
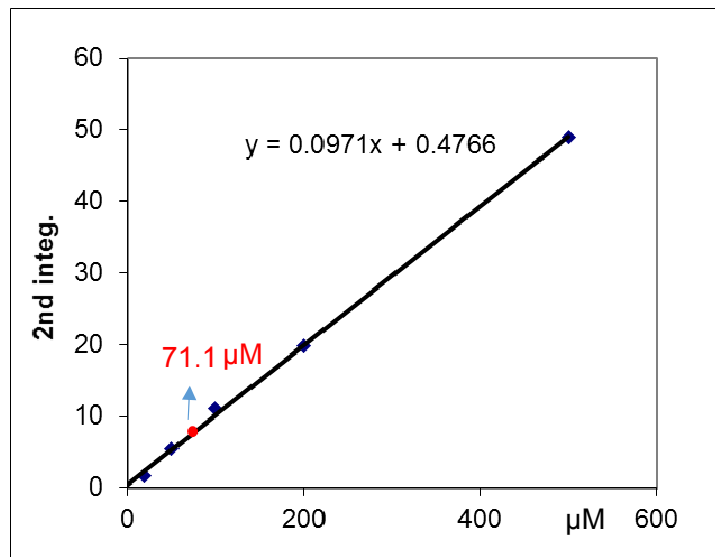


Fig. S8 Estimation of the spin concentration of **12**.



MTSL (1-oxyl-2,2,5,5- tetramethyl- Δ 3-pyrroline-3-methyl methanethiosulfonate) was used as a standard. A set of dilution with different concentration (20, 50, 100, 200, and 500 μ M) was used as spin concentration estimation; the spin concentration (red spot •) of **12** at a concentration of 2 mM in MeOH was estimated to be 71.1 μ M, indicating a ratio of around 3.6%.

Fig. S9 Phylogenetic analysis of XiaK with other flavoenzymes.

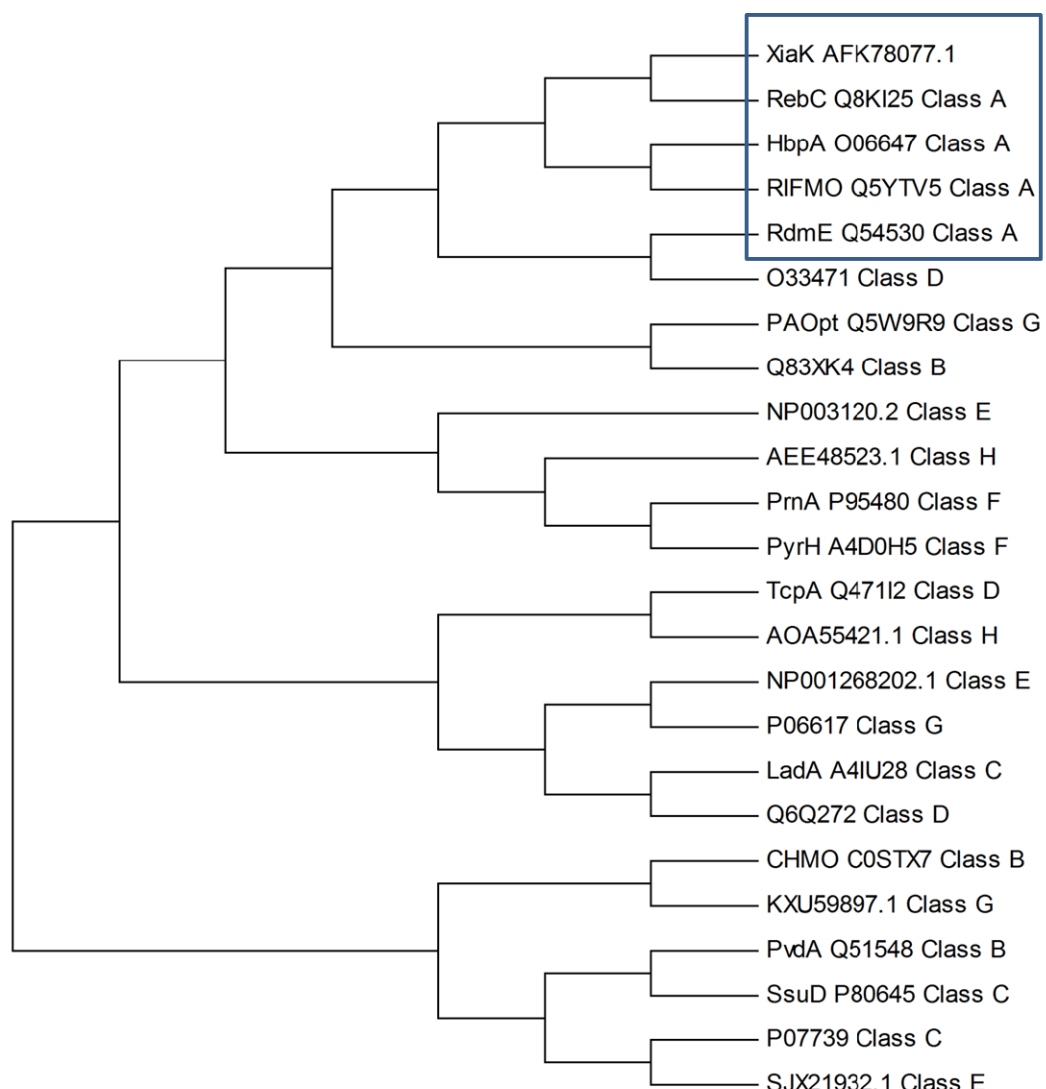
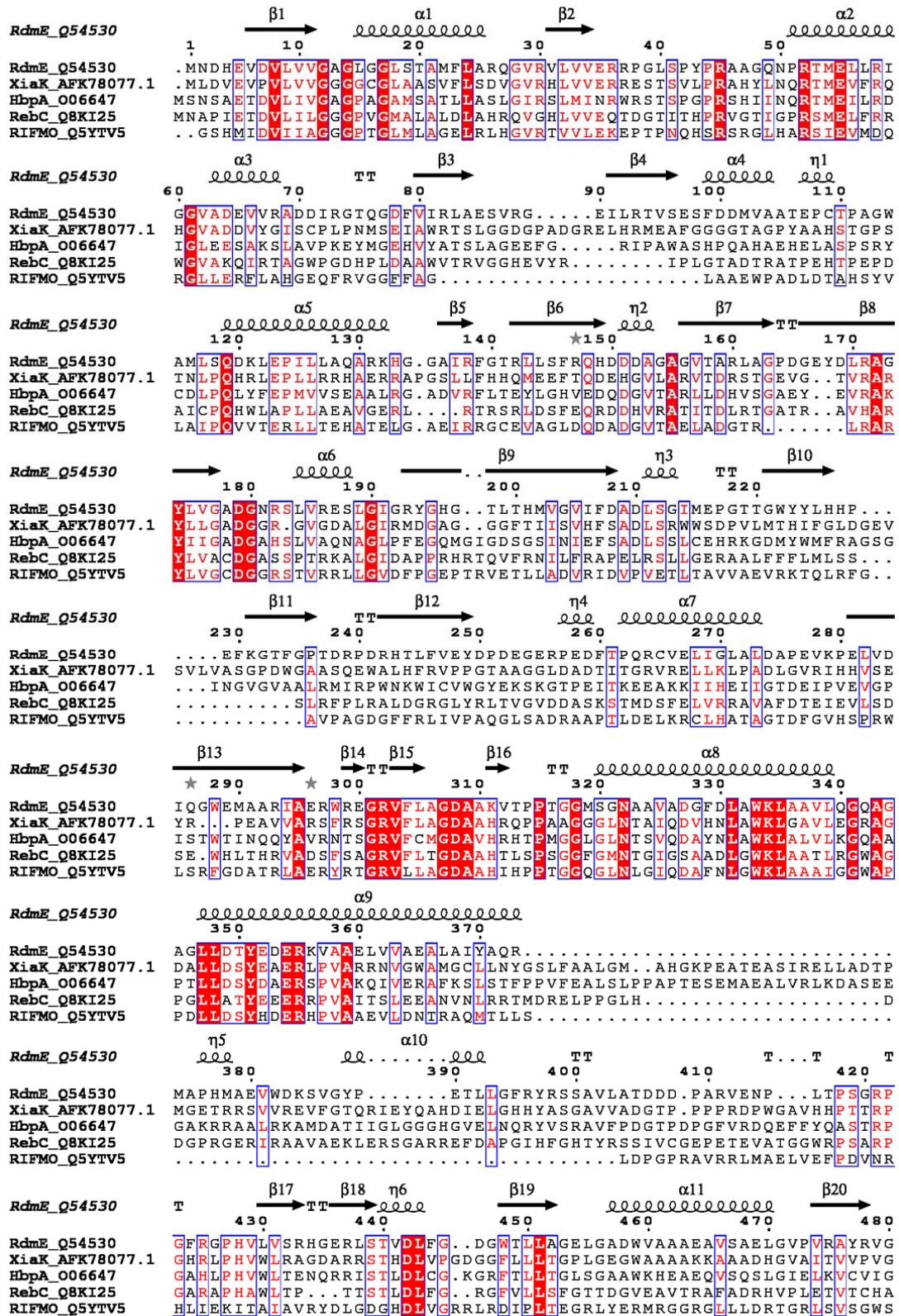


Fig. S10 Comparison of well aligned XiaK structure model and the crystal structures of Class A flavoprotein monooxygenases



The 3D-model of XiaK (cyan cartoon) was build by I-TASSER online server and structures alignment was processed with Pymol. A survey of the Protein Data Bank shows that the closes structural homologs of XiaK to be RdmE (yellow, PDB code 3IHG¹⁶), HbpA (salmon, PDB code 5BRT¹⁷), RifMO (magenta, PDB code 5KOW¹⁸) and RebC (grey, PDB code 2R0C¹⁹), which are all class A flavoprotein monooxygenases. According to Phylogenetic analysis, sequence and structural comparisions, XiaK is considered to be a member of class A flavoprotein monooxygenases.²⁰⁻²²

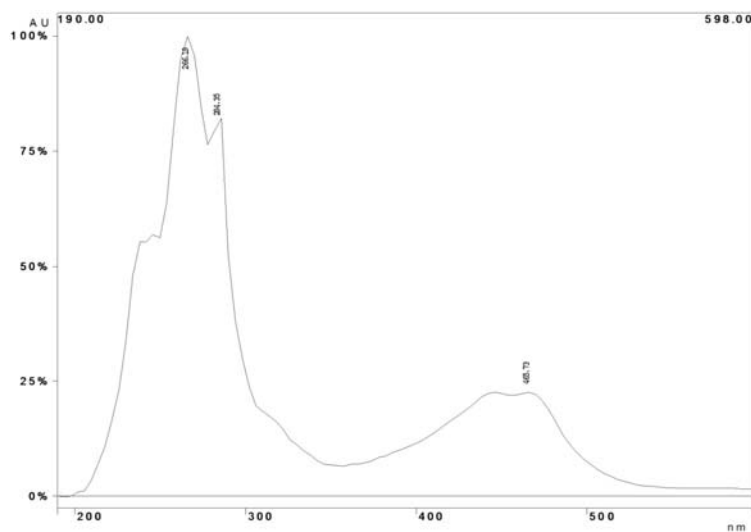
Fig. S11 Sequence Comparison of XiaK and four class A flavoprotein monooxygenases.



XiaK consists of a conserved motif of glycine residues GXGXXG and secondary structure of $\beta\alpha\beta$ -Rossmann fold, which are characteristics of FAD binding domain.

Fig. S12 UV-Vis and HRESIMS spectra of **16**.

(A) UV-vis spectrum of **16**.



(B) HRESIMS spectrum of **16**.

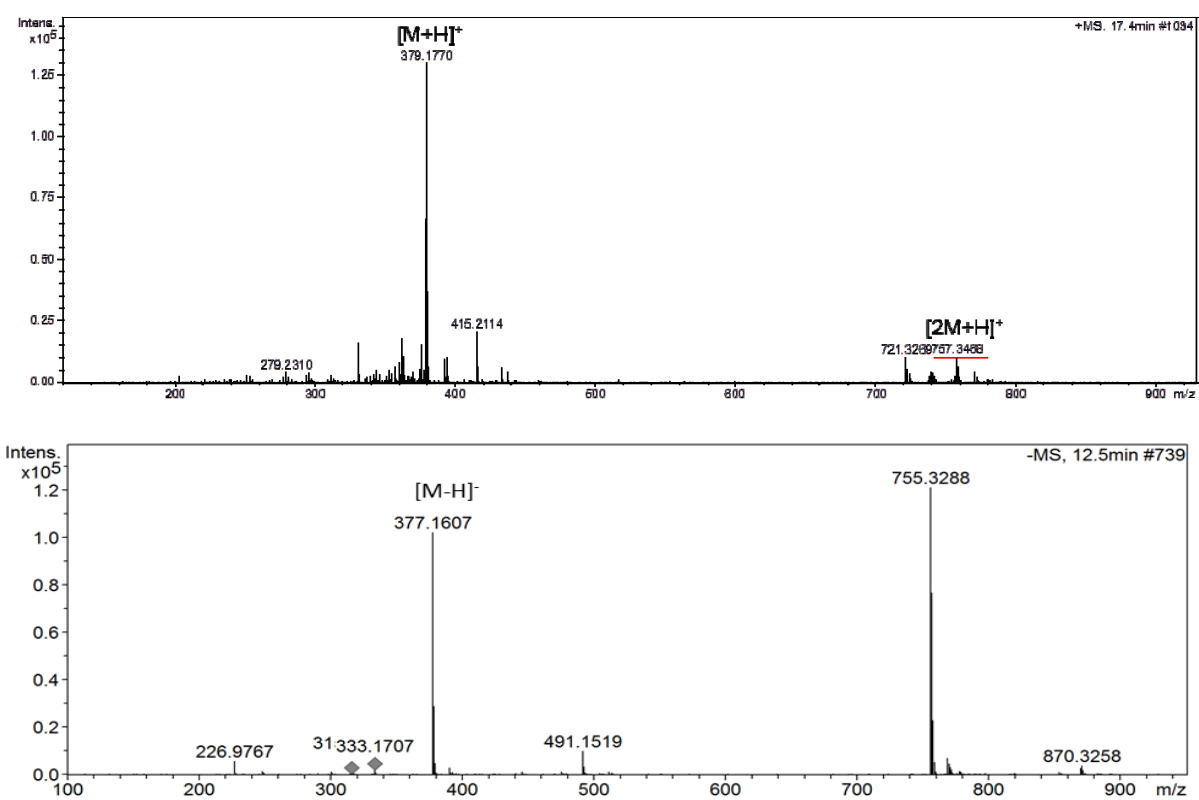


Fig. S13 Comparison of UV-vis spectra of **1**, **17** and **18**.

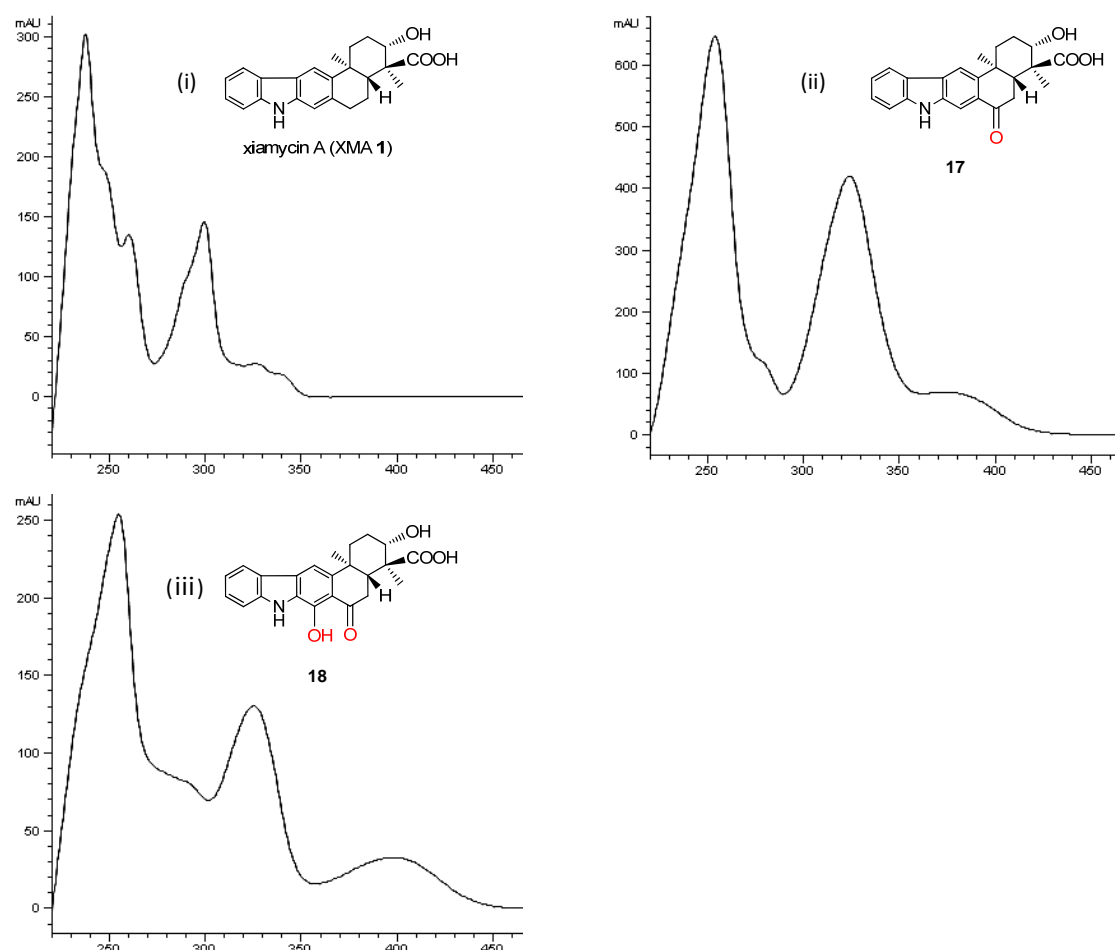
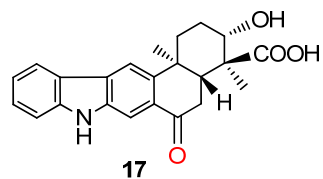


Fig. S14 The spectral data of **17** (600 MHz for ^1H NMR, 150 MHz for ^{13}C NMR, CD_3OD)

(A) The HRESIMS spectrum of **17**.



Chemical Formula: $\text{C}_{23}\text{H}_{23}\text{NO}_4$

$[\text{M} - \text{H}]^+$: calcd. 376.1554

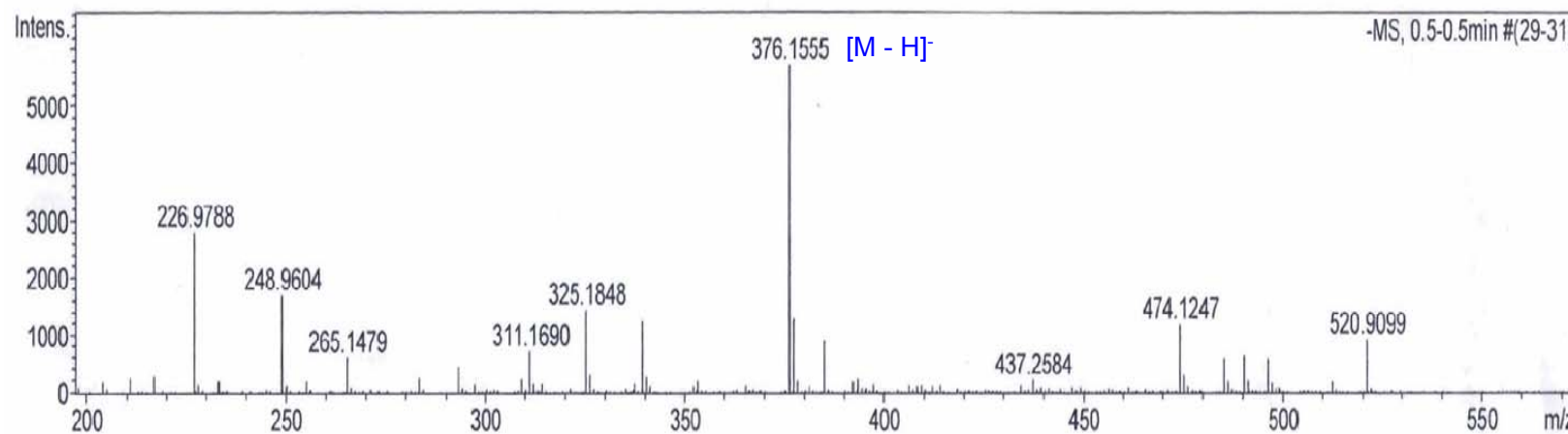


Fig. S14 The spectral data of **17**. (600 MHz for ^1H NMR, 150 MHz for ^{13}C NMR, CD_3OD)

(B) The ^1H -NMR spectrum of **17**.

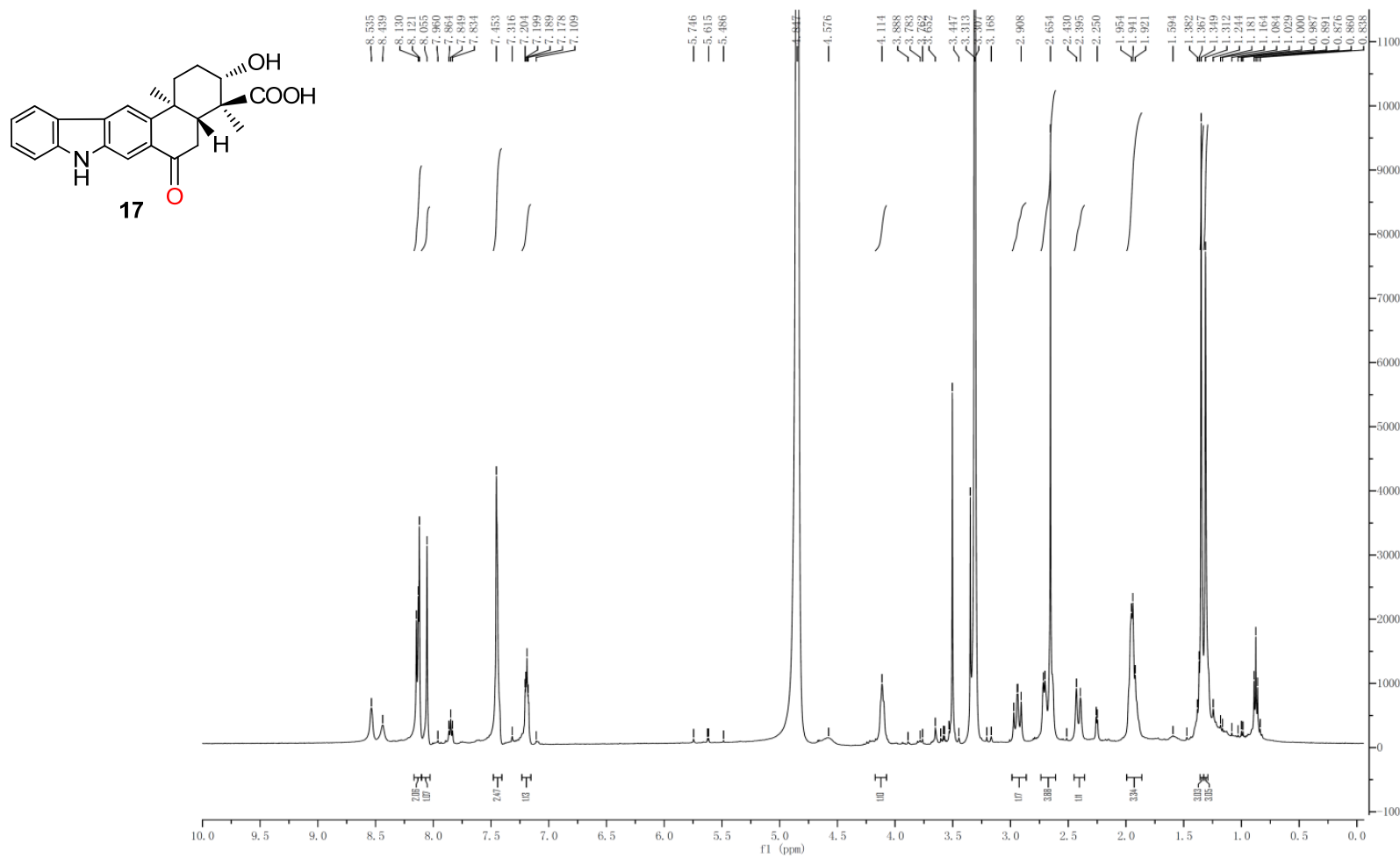


Fig. S14 The spectral data of **17** (600 MHz for ^1H NMR, 150 MHz for ^{13}C NMR, CD_3OD)

(C) The ^{13}C -NMR spectrum of **17**.

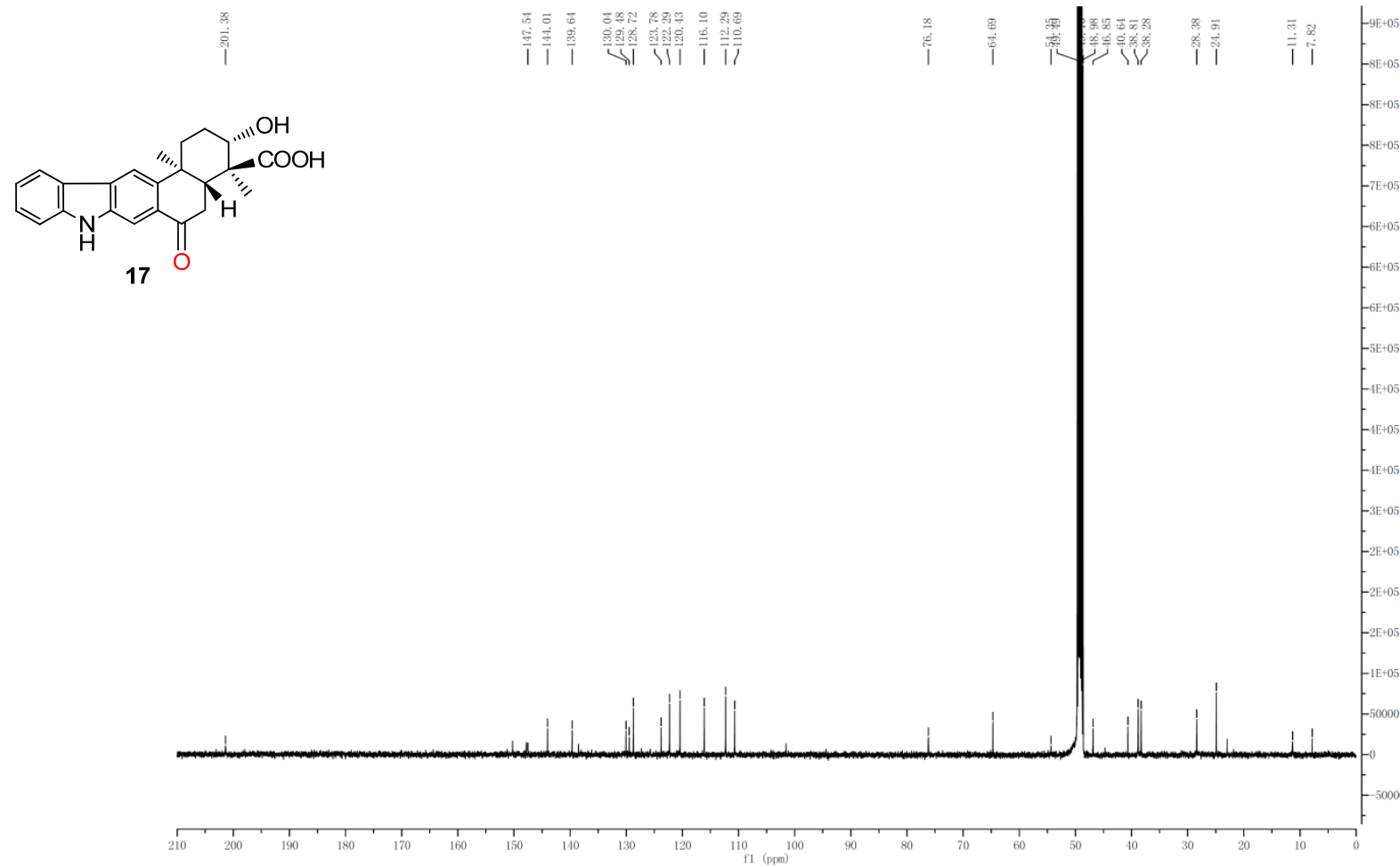


Fig. S14 The spectral data of **17** (600 MHz for ^1H NMR, 150 MHz for ^{13}C NMR, CD_3OD)

(D) The DEPT135 spectrum of **17**.

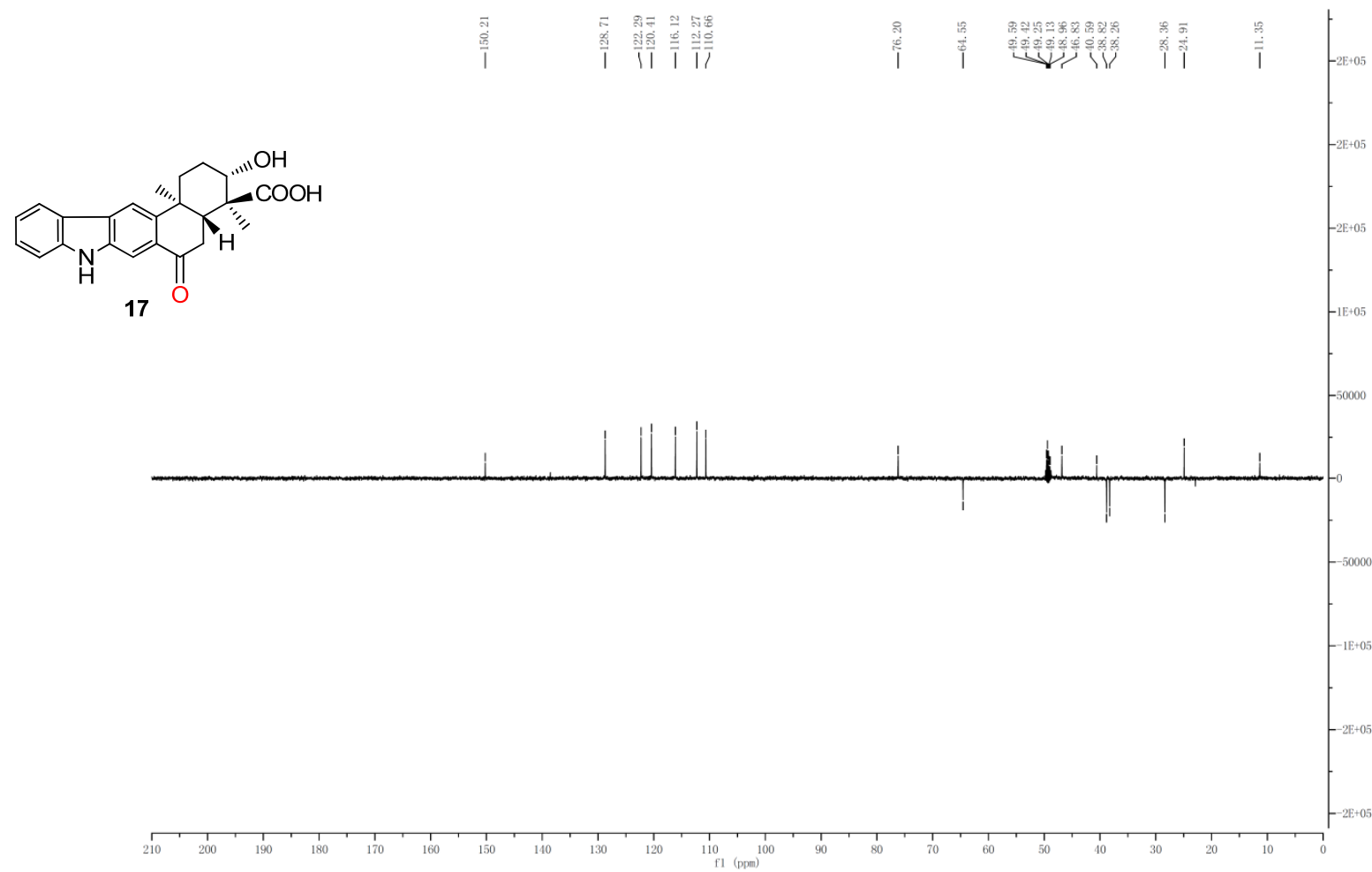


Fig. S14 The spectral data of **17** (600 MHz for ^1H NMR, 150 MHz for ^{13}C NMR, CD_3OD)

(E) The HSQC spectrum of **17**

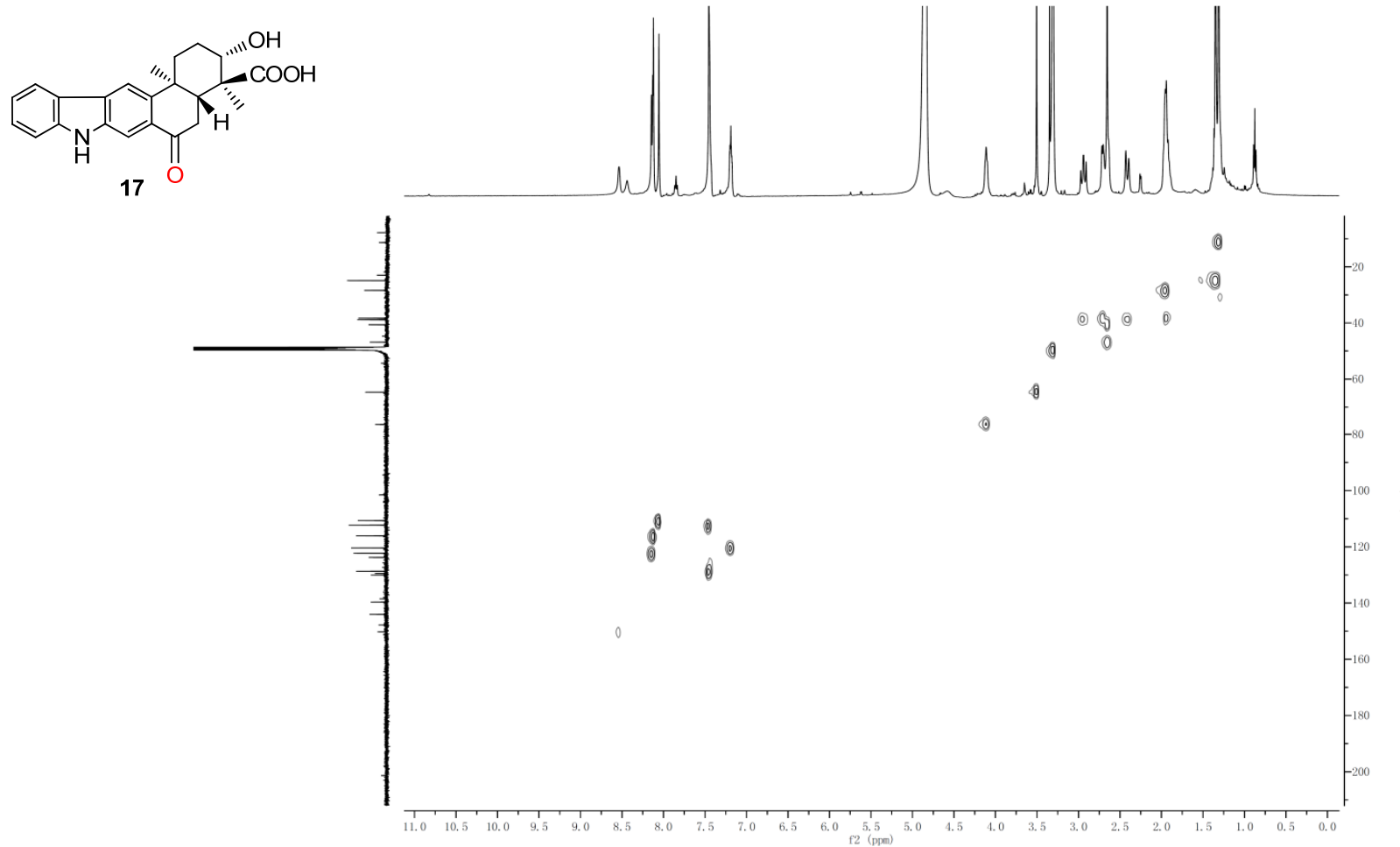


Fig. S14 The spectral data of **17** (600 MHz for ^1H NMR, 150 MHz for ^{13}C NMR, CD_3OD)

(F) The ^1H - ^1H COSY spectrum of **17**

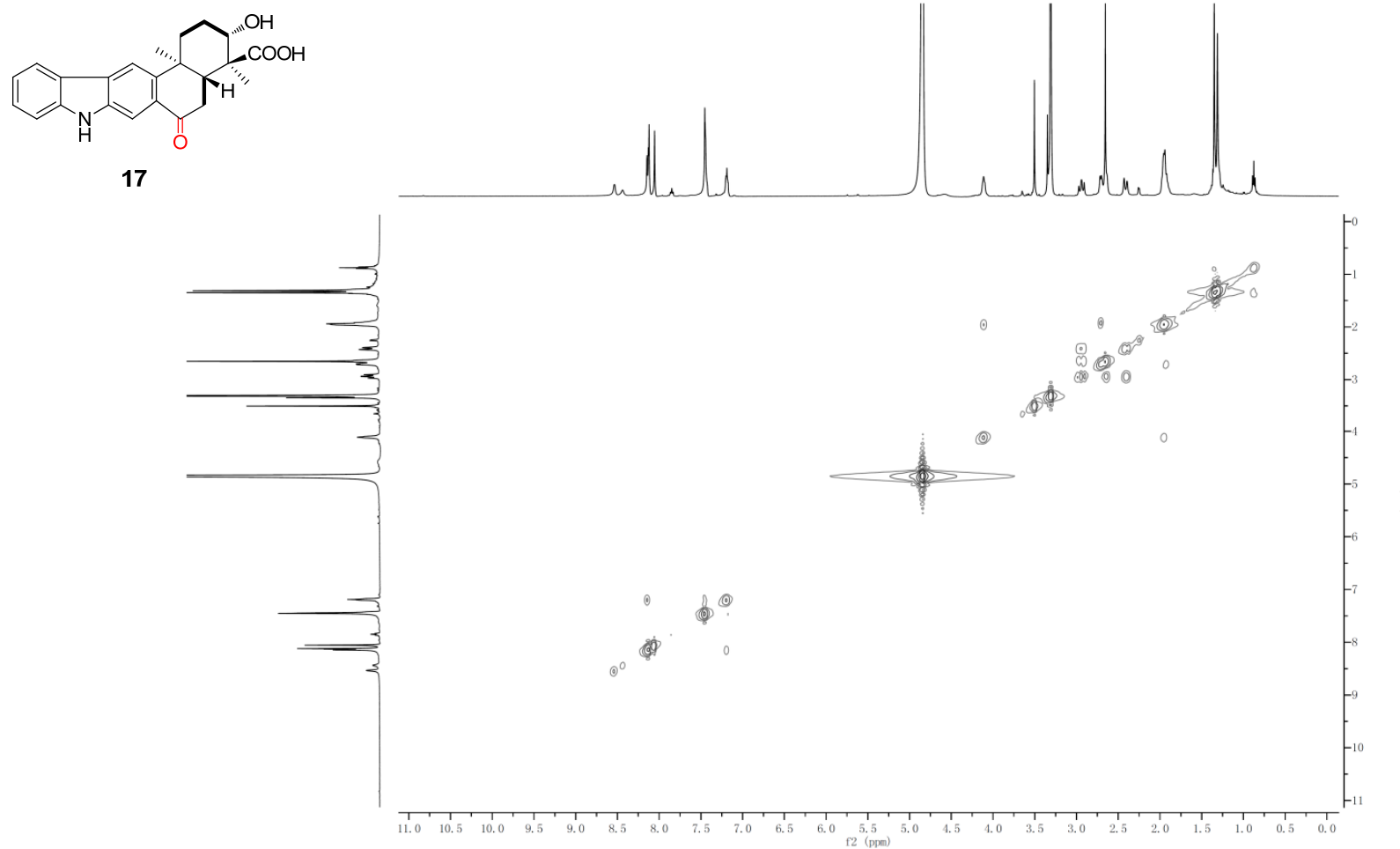


Fig. S14 The spectral data of **17** (600 MHz for ^1H NMR, 150 MHz for ^{13}C NMR, CD_3OD)

(G) The HMBC spectrum of **13**

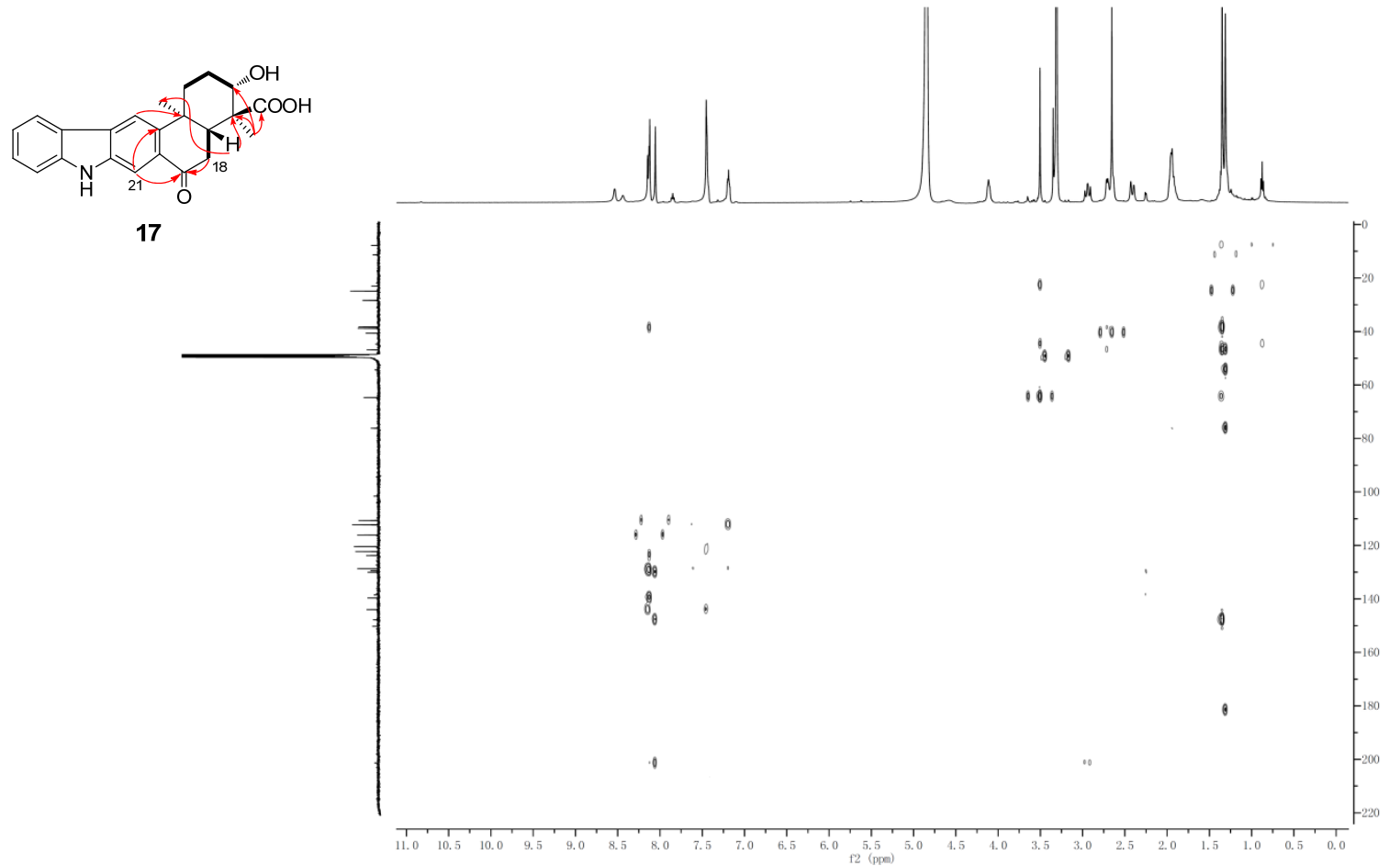
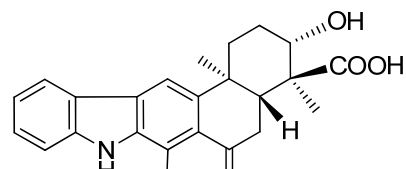


Fig. S15 The spectral data of **18** (600 MHz for ^1H NMR, 150 MHz for ^{13}C NMR, CD_3OD)

(A) The HRESIMS spectrum of **18**.



18

Chemical Formula: $\text{C}_{23}\text{H}_{23}\text{NO}_5$

[$\text{M} - \text{H}$] $^-$: calcd. 392.1503

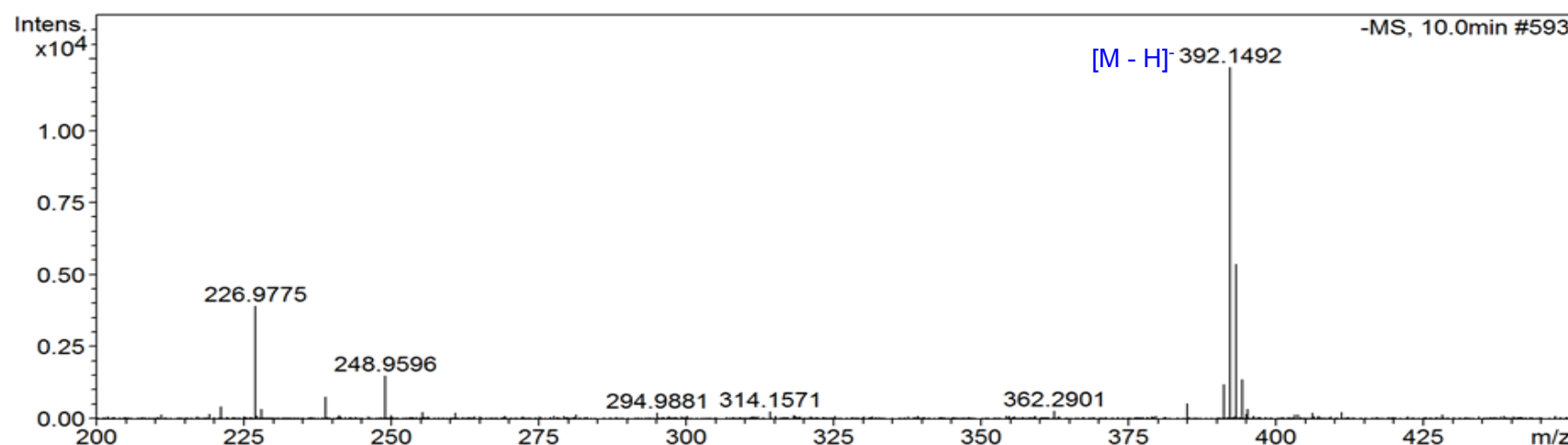


Fig. S15 The spectral data of **18** (600 MHz for ^1H NMR, 150 MHz for ^{13}C NMR, CD_3OD)
(B) The ^1H -NMR spectrum of **18**.

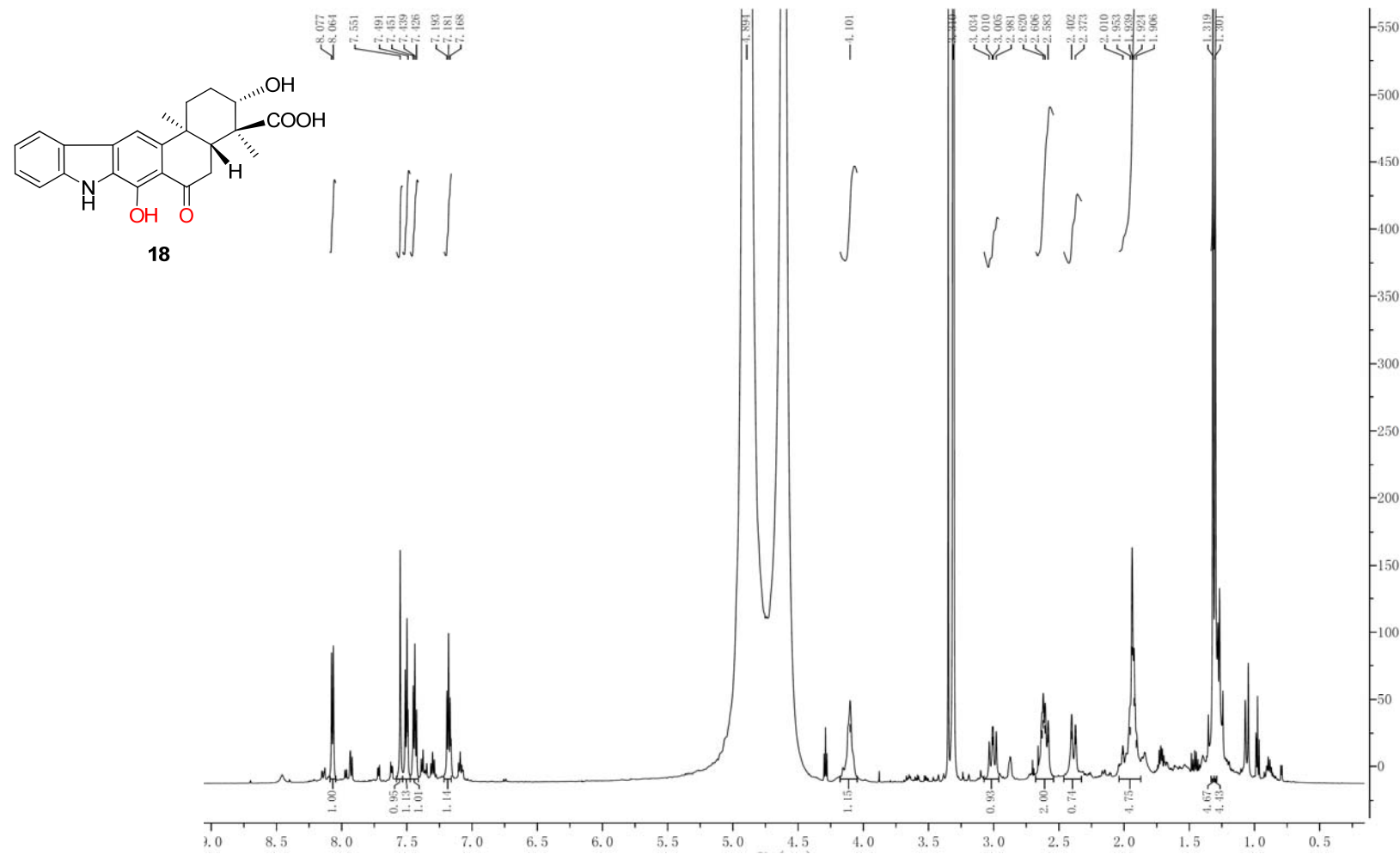


Fig. S15 The spectral data of **18** (600 MHz for ^1H NMR, 150 MHz for ^{13}C NMR, CD_3OD)

(C) The ^{13}C -NMR spectrum of **18**.

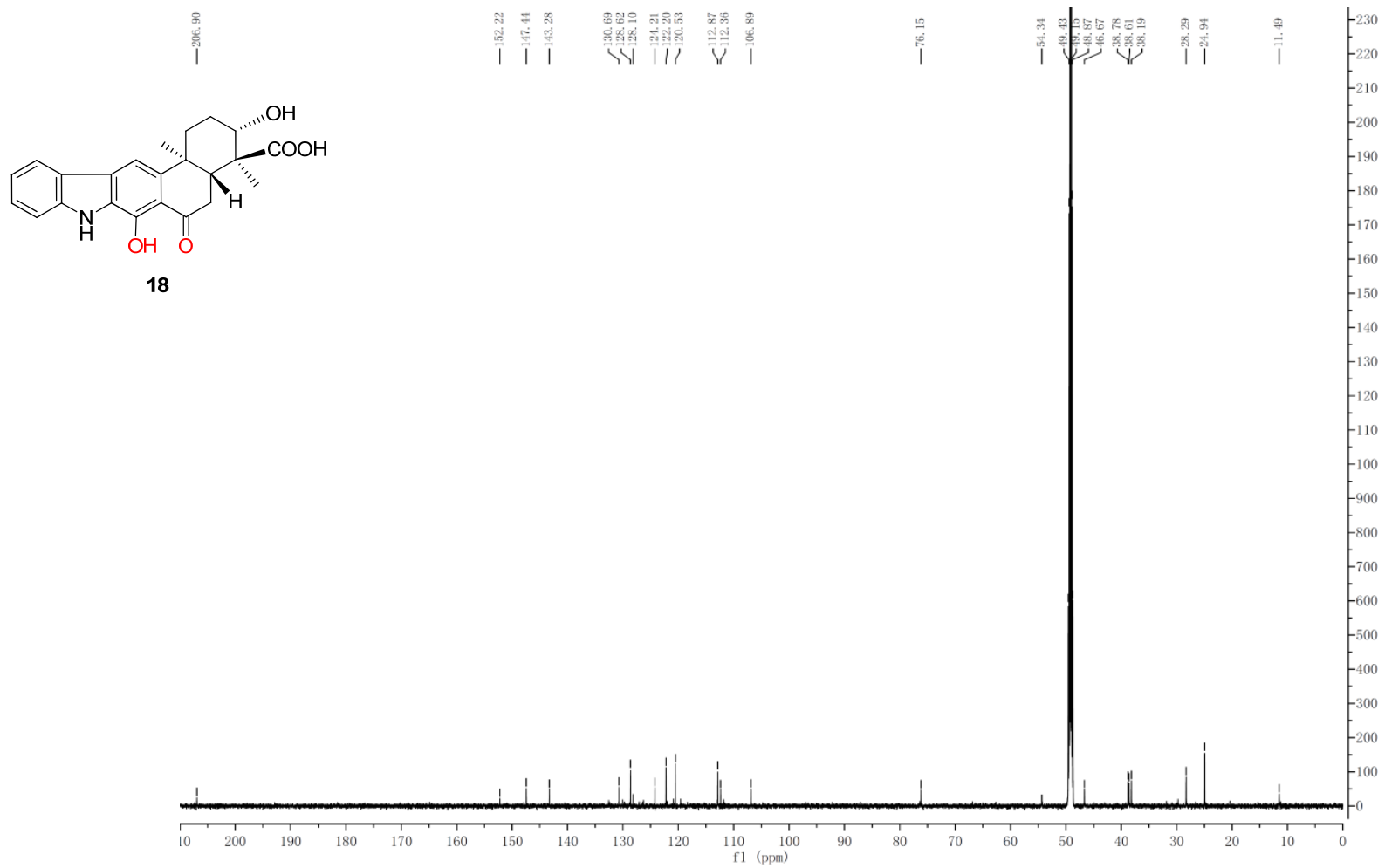


Fig. S15 The spectral data of **18** (600 MHz for ^1H NMR, 150 MHz for ^{13}C NMR, CD_3OD)
(D) The DEPT135 spectrum of **18**.

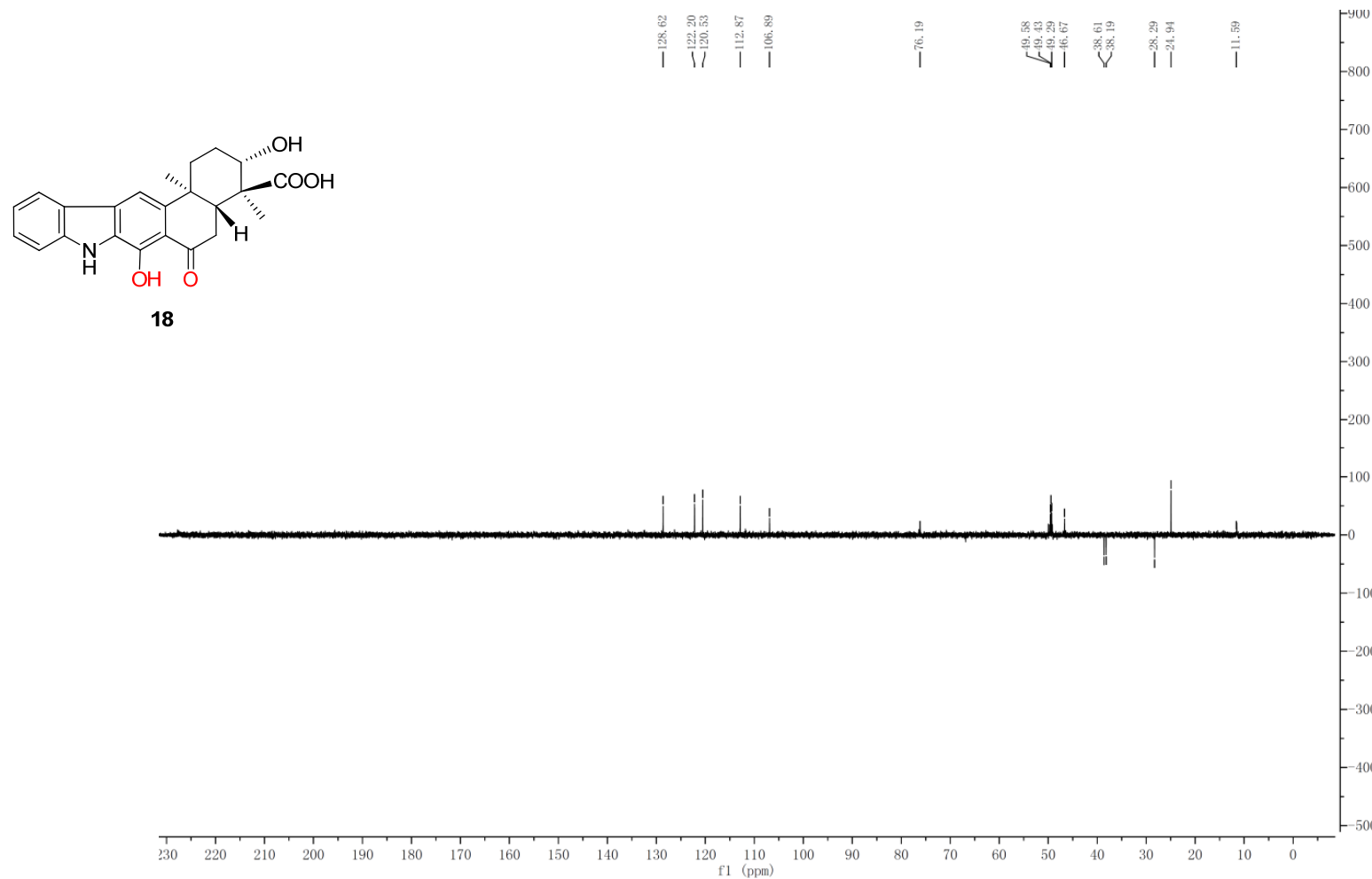


Fig. S15 The spectral data of **18** (600 MHz for ^1H NMR, 150 MHz for ^{13}C NMR, CD_3OD)
(E) The HSQC spectrum of **18**.

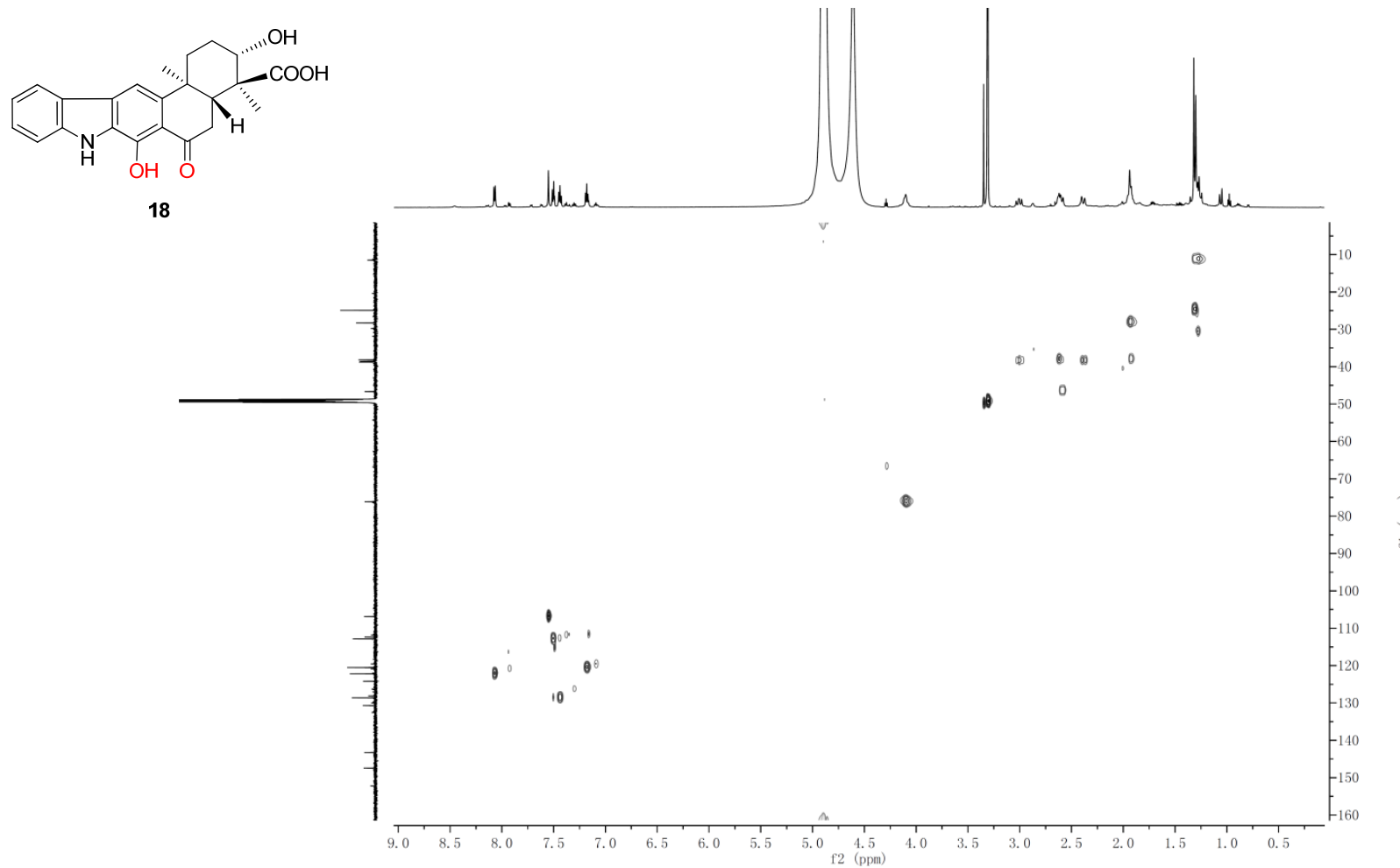


Fig. S15 The spectral data of **18** (600 MHz for ^1H NMR, 150 MHz for ^{13}C NMR, CD_3OD)

(F) The ^1H - ^1H COSY spectrum of **18**.

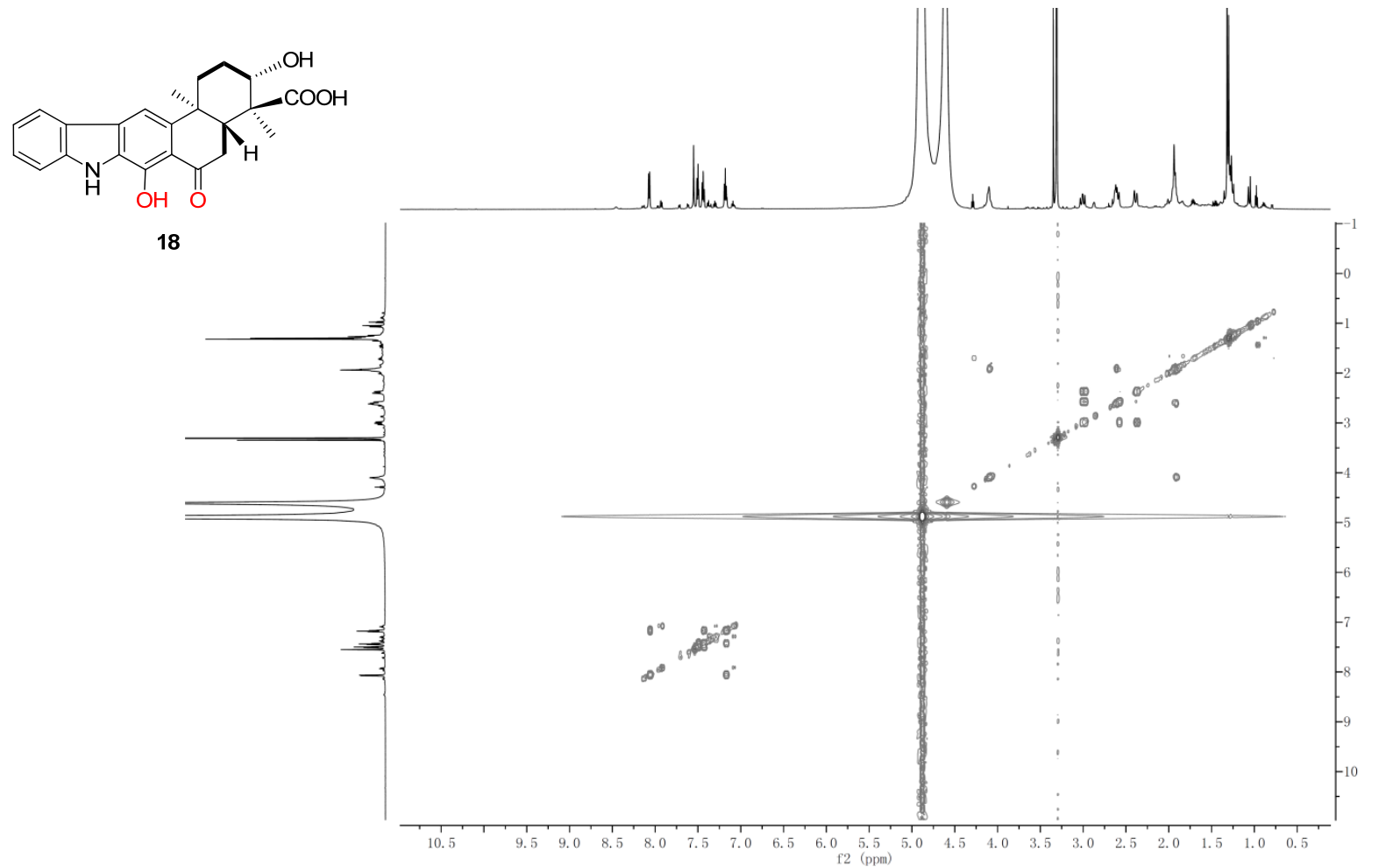


Fig. S15 The spectral data of **18** (600 MHz for ^1H NMR, 150 MHz for ^{13}C NMR, CD_3OD)

(G) The HMBC spectrum of **18**.

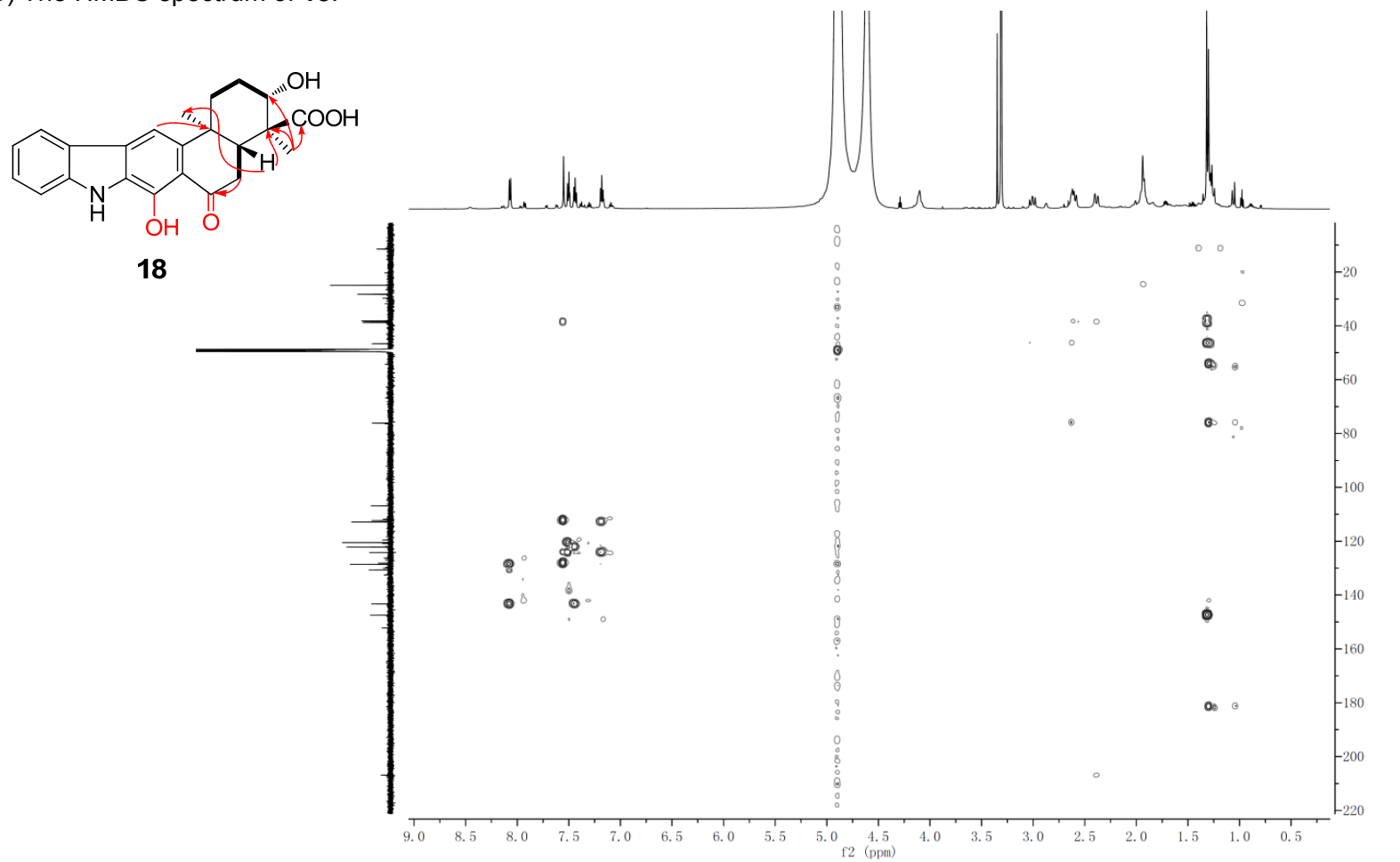


Fig. S16 The spectral data of **19** (600 MHz for ^1H NMR, 150 MHz for ^{13}C NMR, CD_3OD)

(A) The HRESIMS spectrum of **19**

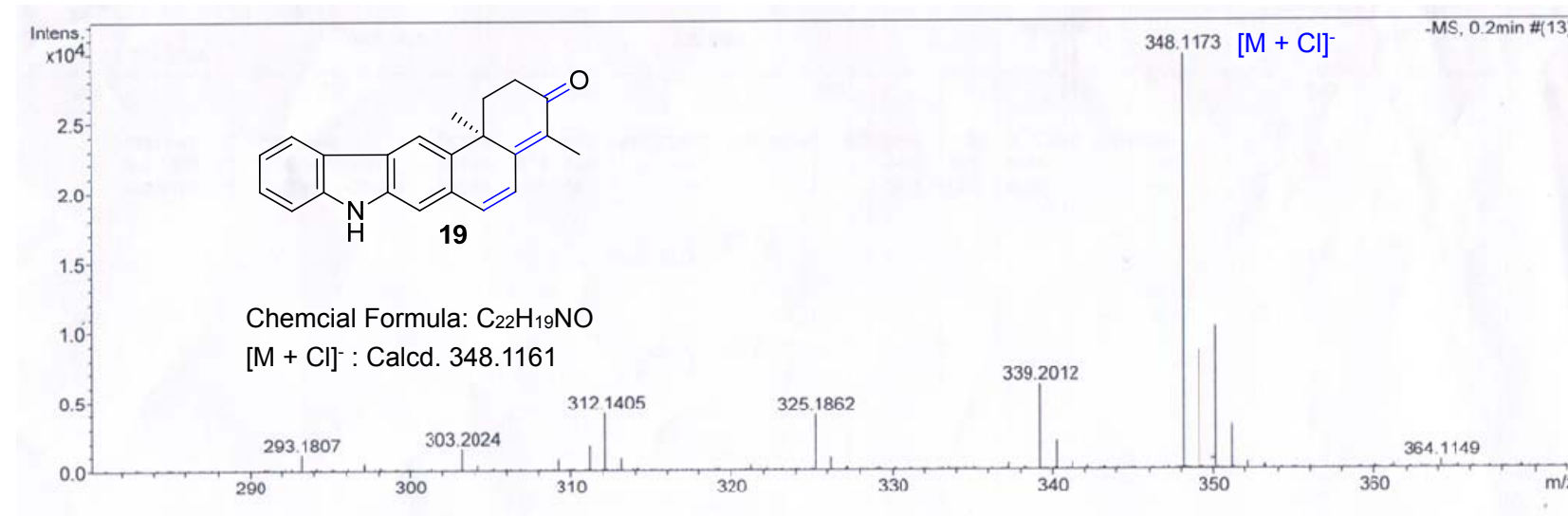


Fig. S16 The spectral data of **19** (600 MHz for ^1H NMR, 150 MHz for ^{13}C NMR, CD_3OD)
(B) The ^1H -NMR spectrum of **19**

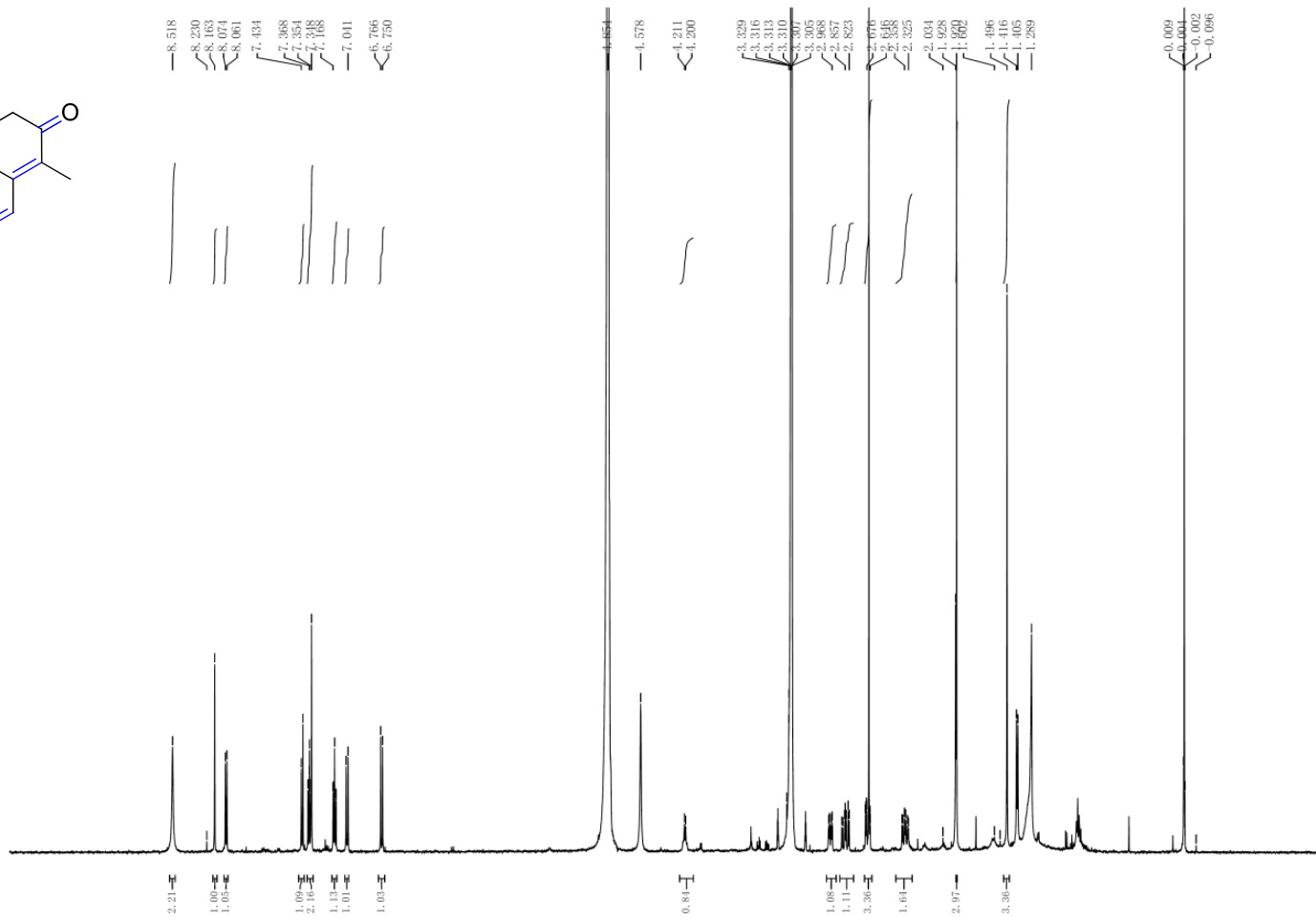
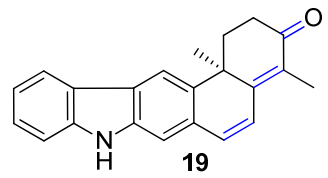


Fig. S16 The spectral data of **19** (600 MHz for ^1H NMR, 150 MHz for ^{13}C NMR, CD_3OD)

(C) The ^{13}C -NMR spectrum of **19**

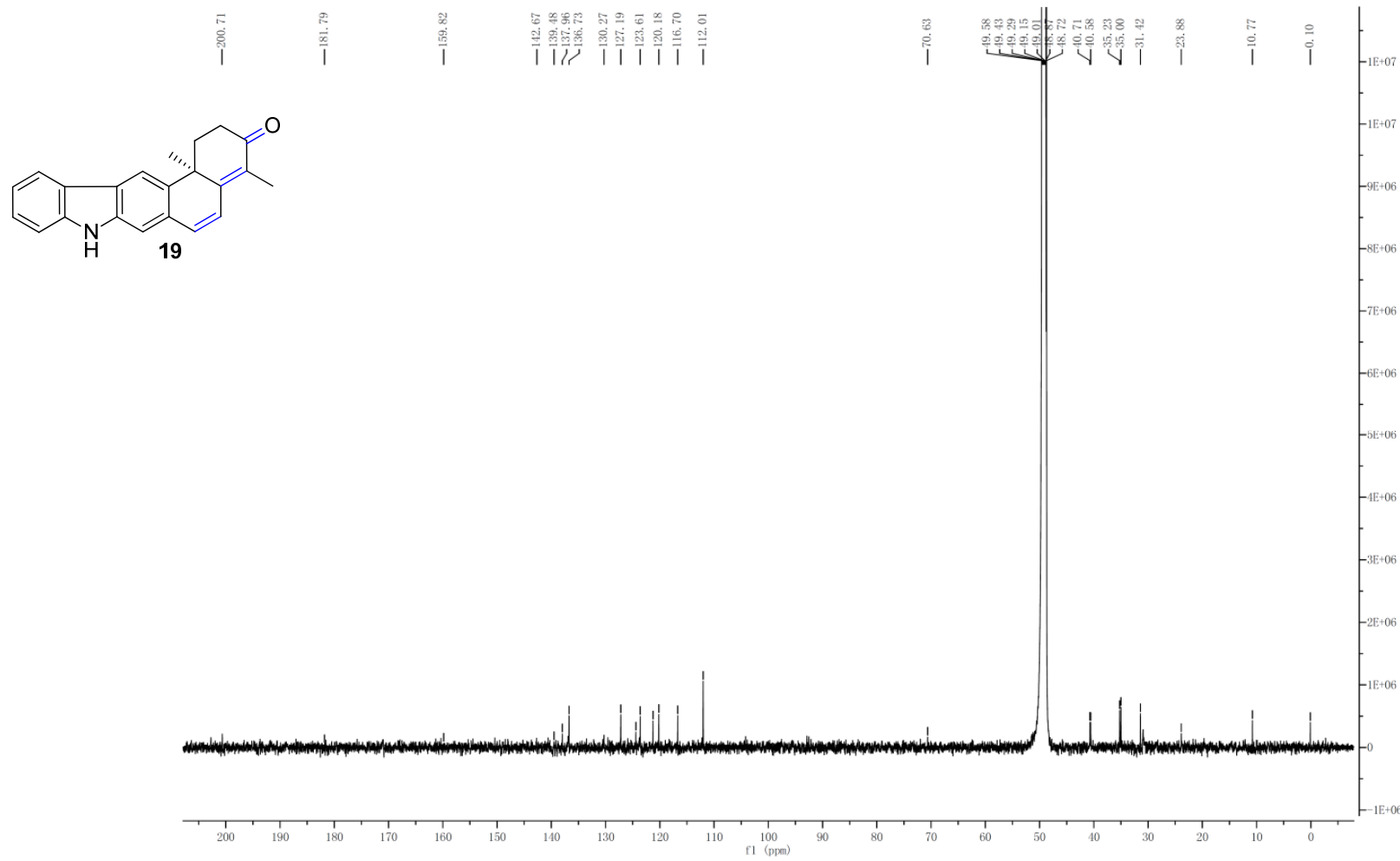


Fig. S16 The spectral data of **19** (600 MHz for ^1H NMR, 150 MHz for ^{13}C NMR, CD_3OD)

(D) The DEPT135 spectrum of **19**

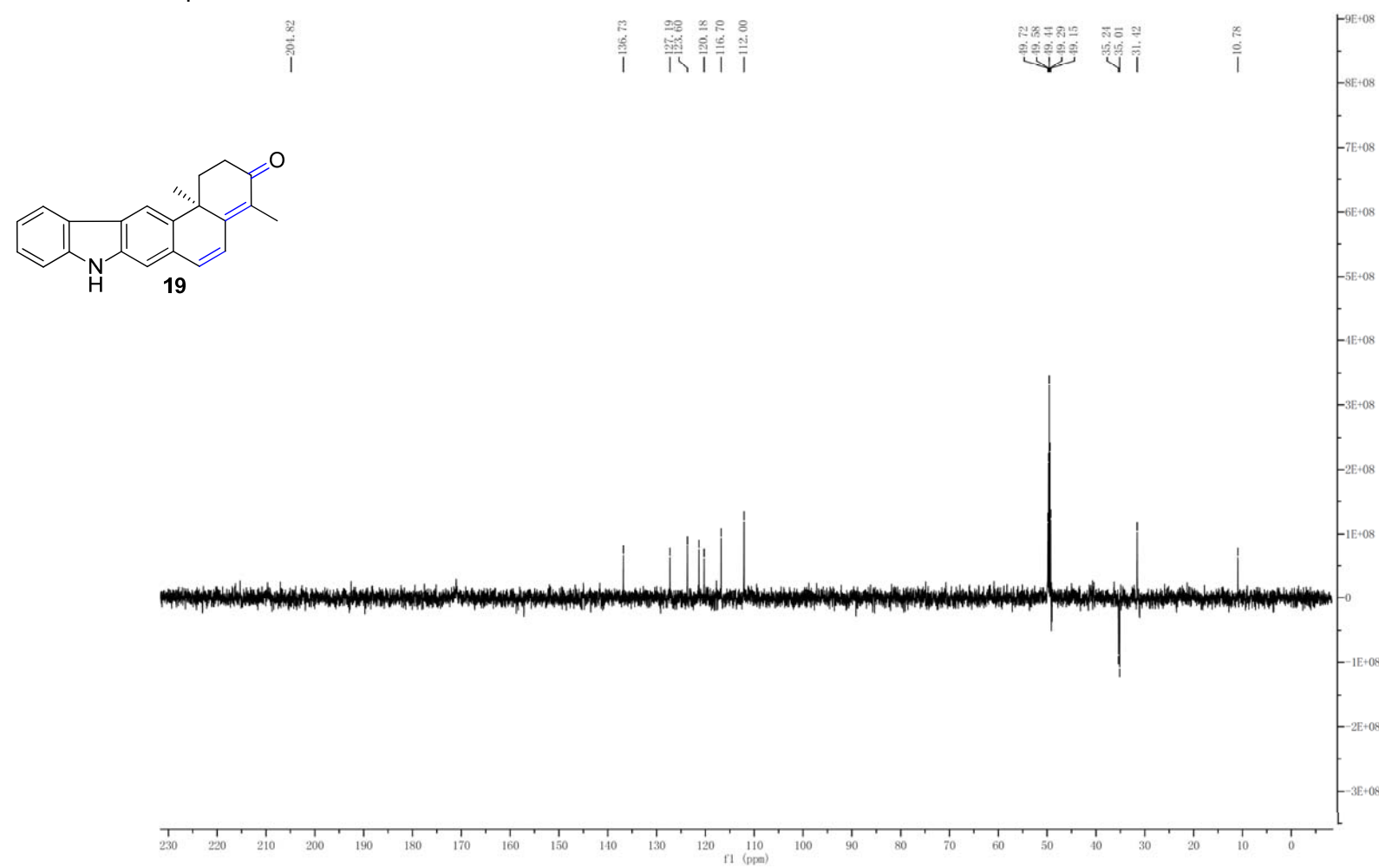


Fig. S16 The spectral data of **19** (600 MHz for ^1H NMR, 150 MHz for ^{13}C NMR, CD_3OD)
(E) The HSQC spectrum of **19**

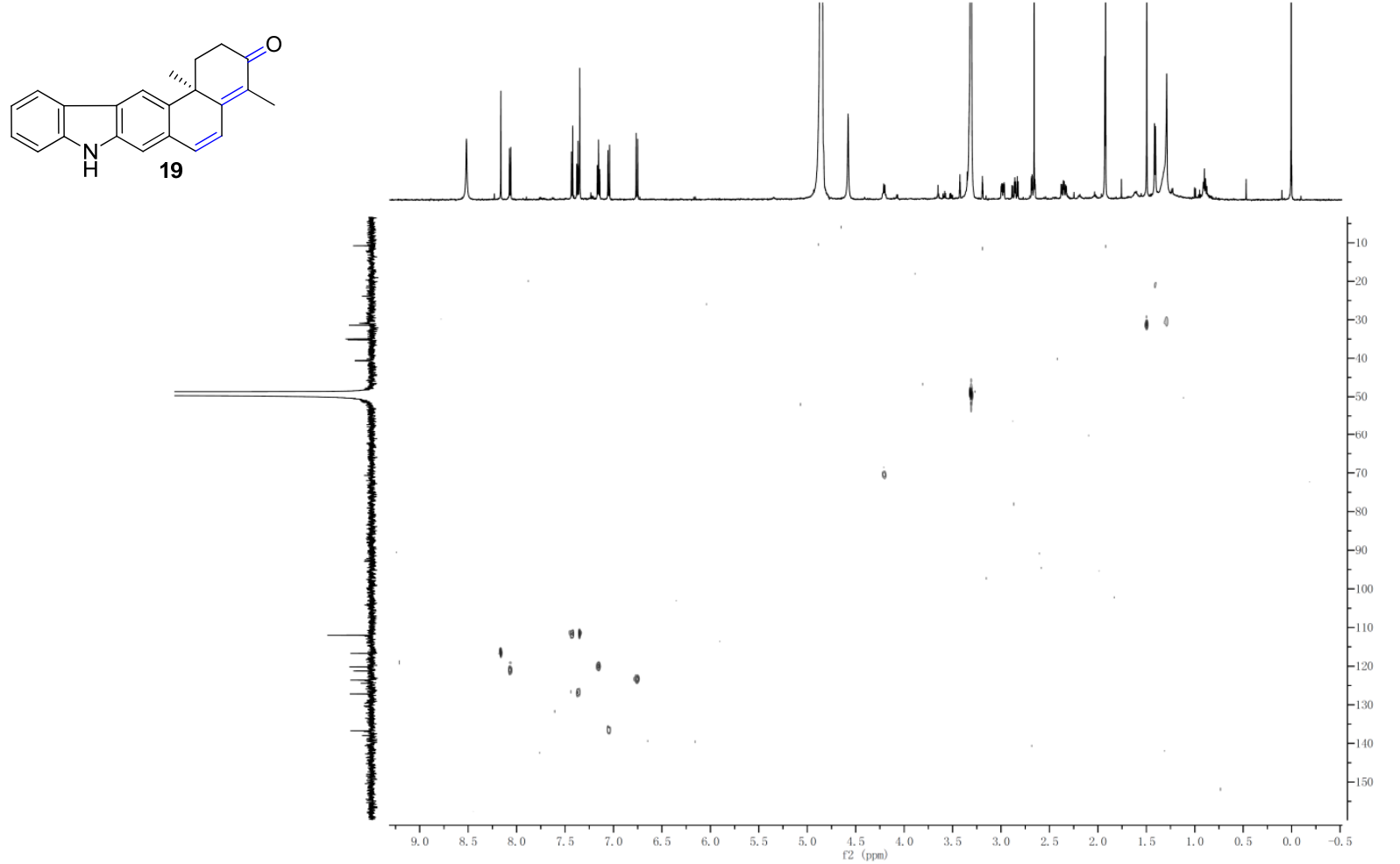


Fig. S16 The spectral data of **19** (600 MHz for ^1H NMR, 150 MHz for ^{13}C NMR, CD_3OD)

(F) The HMQC spectrum of **19**

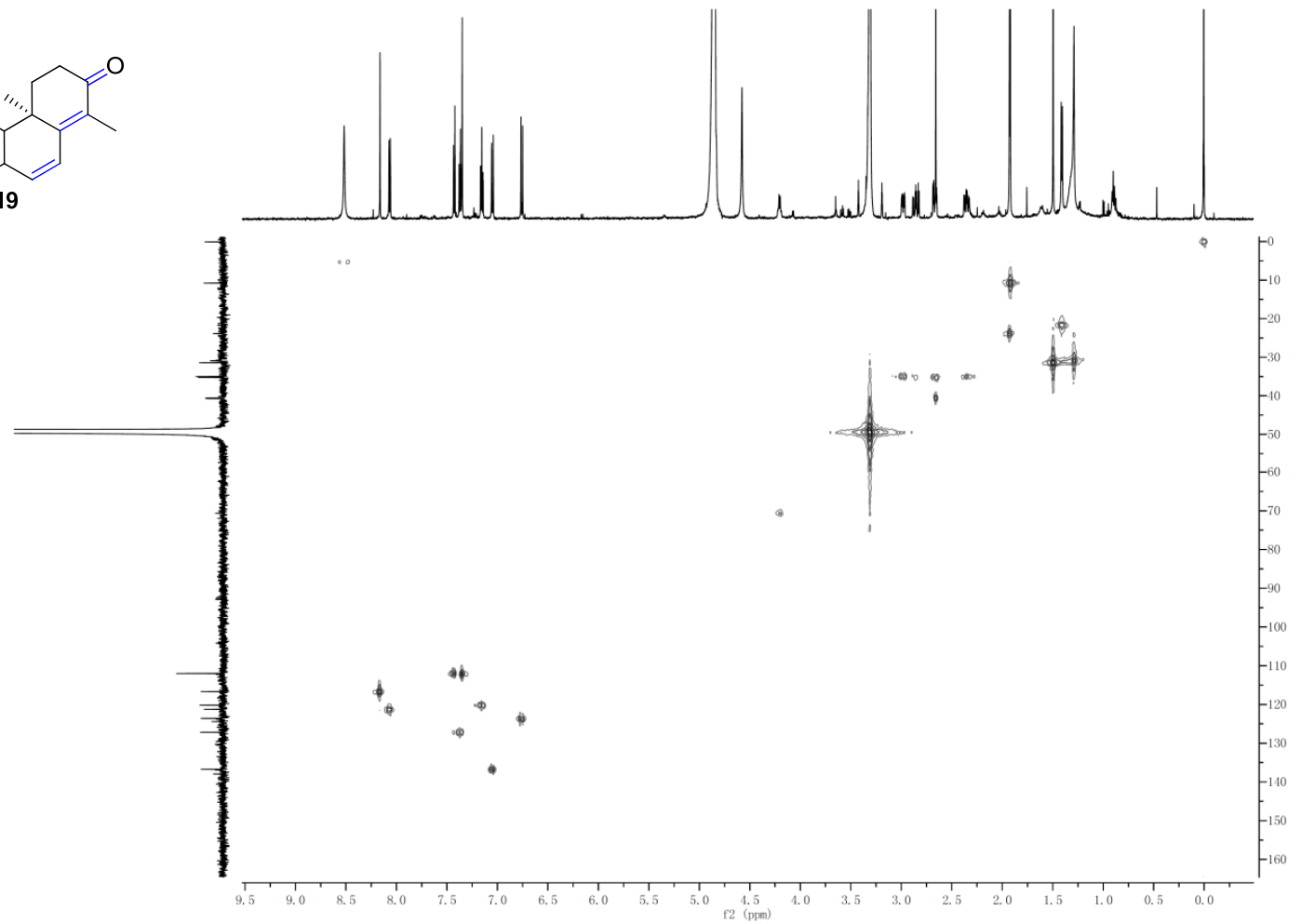
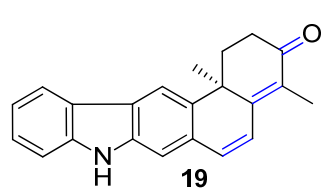


Fig. S16 The spectral data of **19** (600 MHz for ^1H NMR, 150 MHz for ^{13}C NMR, CD_3OD)

(G) The ^1H - ^1H COSY spectrum of **19**

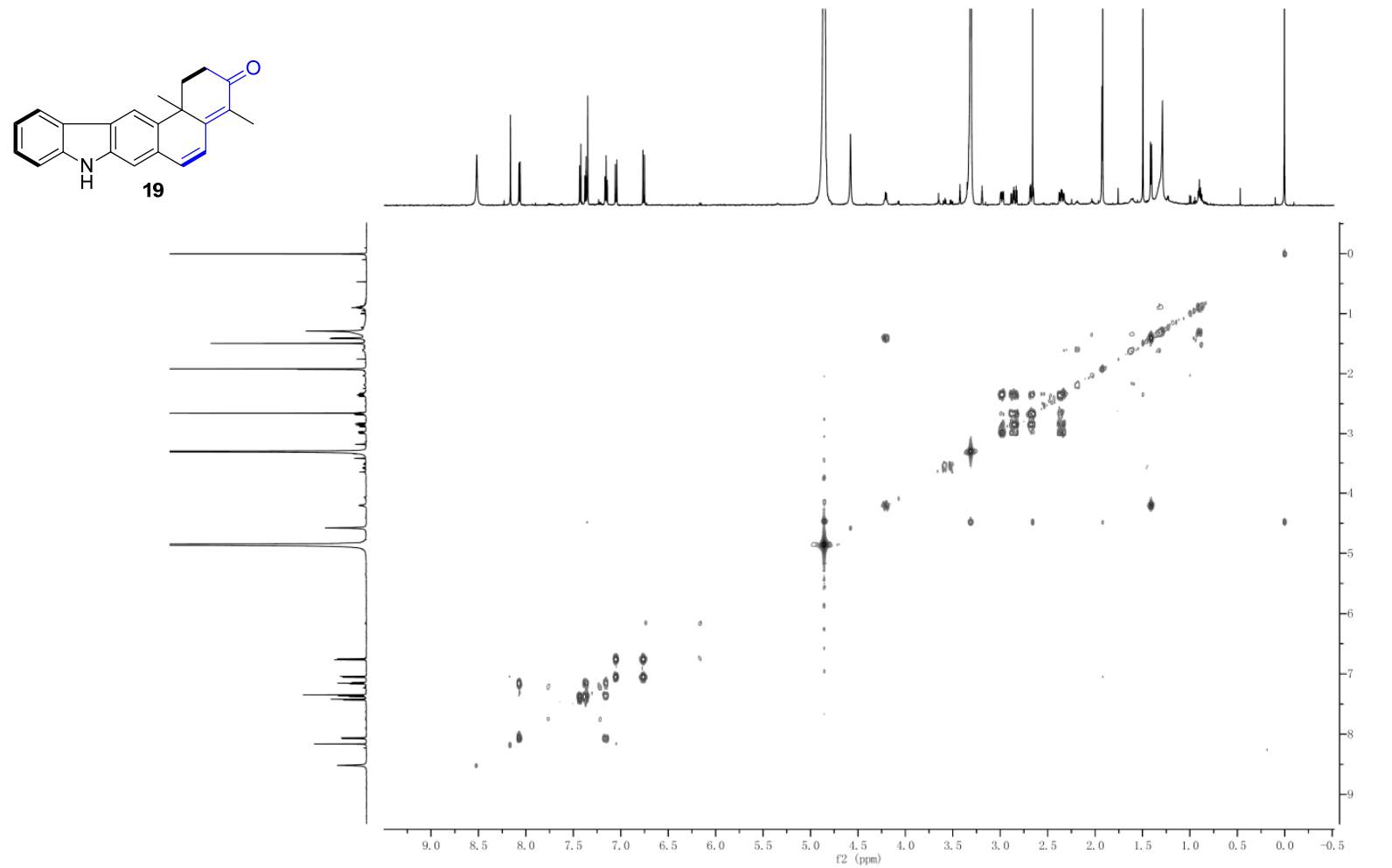


Fig. S16 The spectral data of **19** (600 MHz for ^1H NMR, 150 MHz for ^{13}C NMR, CD_3OD)

(H) The HMBC spectrum of **19**

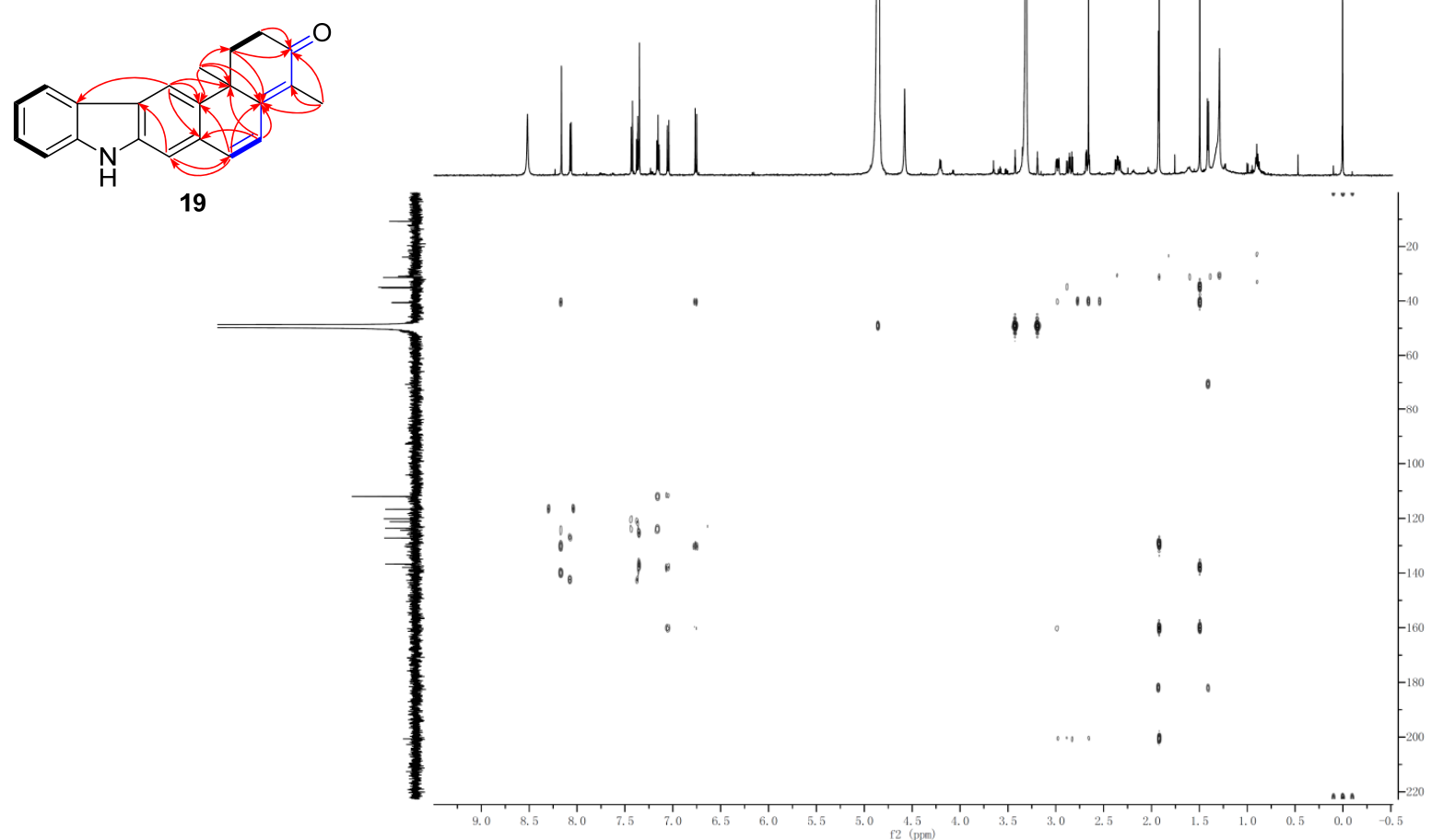
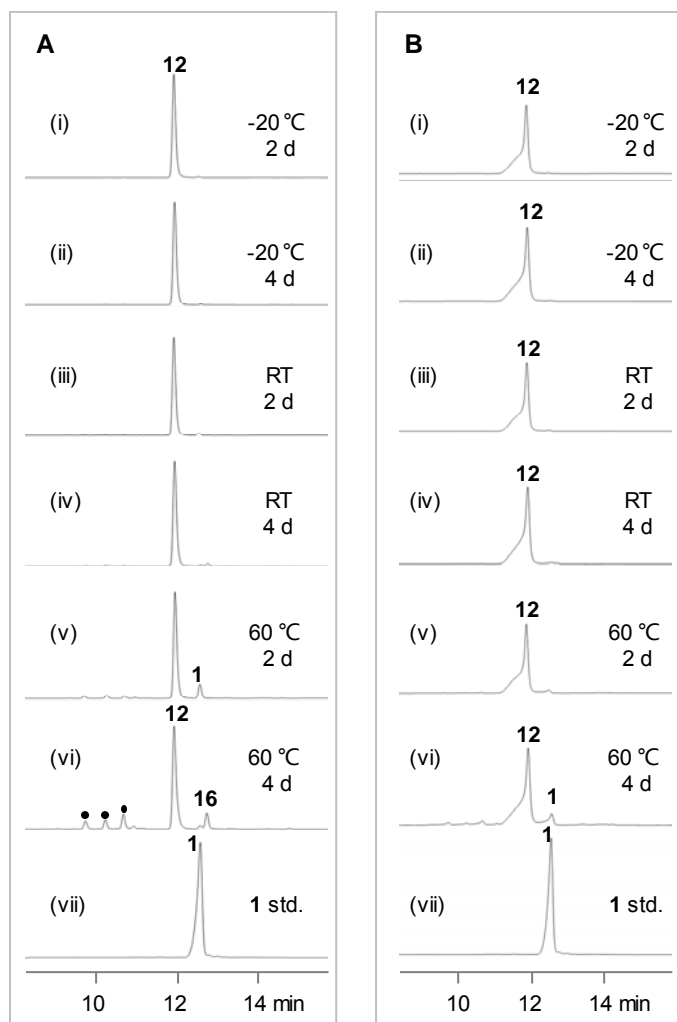
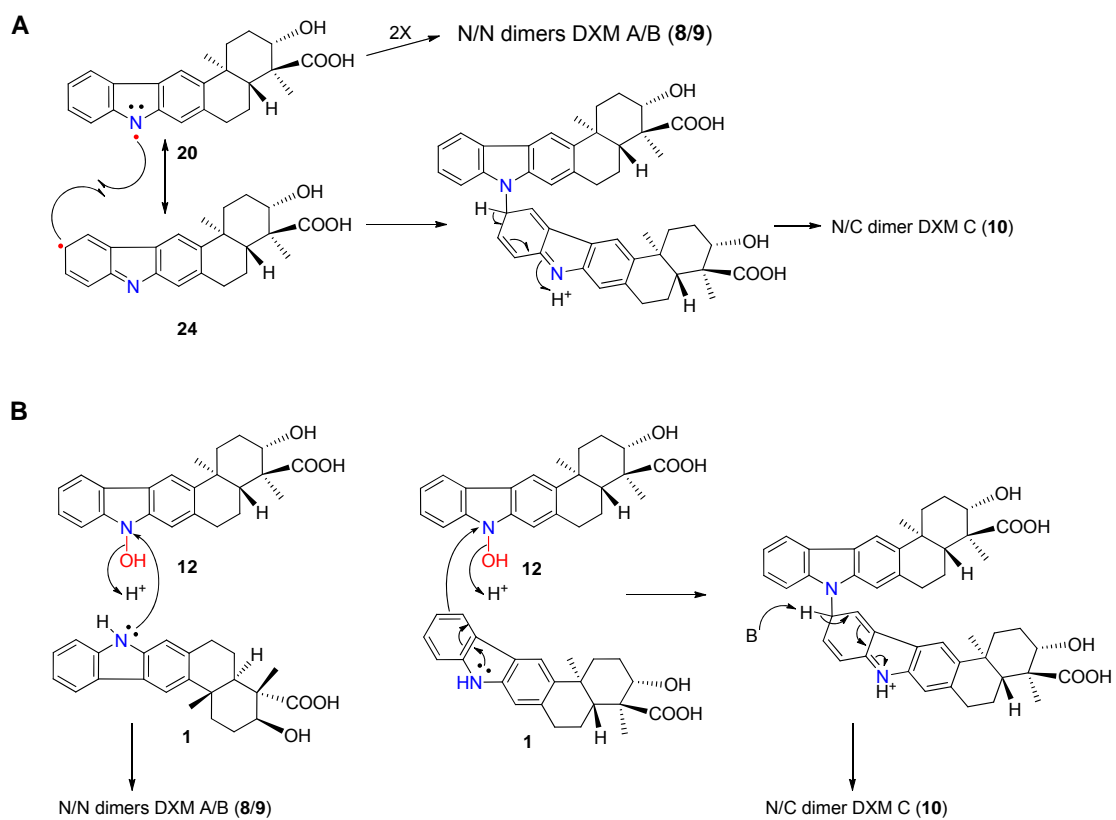


Fig. S17 Stability of compounds **12** stored in organic solvents.



(A): **NOXM (12)** dissolved in $\text{H}_2\text{O}/\text{AcN}$ (1:1, v/v); (B): **12** dissolved in MeOH . (i) stored at -20°C for 2 days; (ii) stored at -20°C for 4 days; (iii) stored at room temperature for 2 days; (iv) stored at room temperature for 4 days; (v) incubated at 60°C for 2 days; (vi) incubated at 60°C for 4 days; (vii) XMA (**1**) standard; the filled black circles (●) denote multiple XMA-related products which have not been isolated for structure elucidation.

Fig. S18 The hypothesized mechanism for the formation of DXMs A-C (**8-10**).



Supplementary Reference

1. D. J. MacNeil, K. M. Gewain, C. L. Ruby, G. Dezeny, P. H. Gibbons and T. MacNeil, *Gene*, 1992, **111**, 61-68.
2. H. Zhou, Y. Wang, Y. Yu, T. Bai, L. Chen, P. Liu, H. Guo, C. Zhu, M. Tao and Z. Deng, *Curr. Microbiol.*, 2011.
3. H. Li, Q. Zhang, S. Li, Y. Zhu, G. Zhang, H. Zhang, X. Tian, S. Zhang, J. Ju and C. Zhang, *J. Am. Chem. Soc.*, 2012, **134**, 8996-9005.
4. K. A. Datsenko and B. L. Wanner, *Proc. Natl. Acad. Sci. U. S. A.*, 2000, **97**, 6640-6645.
5. M. S. B. Paget, L. Chamberlin, A. Atrih, S. J. Foster and M. J. Buttner, *J. Bacteriol.*, 1999, **181**, 204-211.
6. M. Bierman, R. Logan, K. O'Brien, E. T. Seno, R. N. Rao and B. E. Schoner, *Gene*, 1992, **116**, 43-49.
7. Y. Zhu, P. Fu, Q. Lin, G. Zhang, H. Zhang, S. Li, J. Ju, W. Zhu and C. Zhang, *Org. Lett.*, 2012, **14**, 2666-2669.
8. K. M. Meneely and A. L. Lamb, *Biochemistry*, 2007, **46**, 11930-11937.
9. J. A. Mayfield, R. E. Frederick, B. R. Streit, T. A. Wencewicz, D. P. Ballou and J. L. DuBois, *J. Biol. Chem.*, 2010, **285**, 30375-30388.
10. C. Binda, R. M. Robinson, J. S. Martin Del Campo, N. D. Keul, P. J. Rodriguez, H. H. Robinson, A. Mattevi and P. Sobrado, *J. Biol. Chem.*, 2015, **290**, 12676-12688.
11. Y. Sugai, Y. Katsuyama and Y. Ohnishi, *Nat. Chem. Biol.*, 2016, **12**, 73-75.
12. Z. D. Huang, K. K. A. Wang and W. A. van der Donk, *Chem. Sci.*, 2016, **7**, 5219-5223.
13. J. Lee and H. M. Zhao, *Angew. Chem., Int. Ed.*, 2006, **45**, 622-625.
14. H. D. Johnson and J. S. Thorson, *J. Am. Chem. Soc.*, 2008, **130**, 17662-17663.
15. Y. S. Choi, H. Zhang, J. S. Brunzelle, S. K. Nair and H. Zhao, *Proc. Natl. Acad. Sci. U. S. A.*, 2008, **105**, 6858-6863.
16. Y. Lindqvist, H. Koskinen, A. Jansson, T. Sandalova, R. Schnell, Z. L. Liu, P. Mantsala, J. Niemi and G. Schneider, *J. Mol. Biol.*, 2009, **393**, 966-977.
17. M. Kanteev, A. Bregman-Cohen, B. Deri, A. Shahar, N. Adir and A. Fishman, *Biochimica Et Biophysica Acta-Proteins and Proteomics*, 2015, **1854**, 1906-1913.
18. L. K. Liu, H. Abdelwahab, J. S. M. Del Campo, R. Mehra-Chaudhary, P. Sobrado and J. J. Tanner, *Journal of Biological Chemistry*, 2016, **291**, 21553-21562.
19. K. S. Ryan, A. R. Howard-Jones, M. J. Hamill, S. J. Elliott, C. T. Walsh and C. L. Drennan, *Proc. Natl. Acad. Sci. U. S. A.*, 2007, **104**, 15311-15316.
20. W. J. H. van Berkel, N. M. Kamerbeek and M. W. Fraaije, *J. Biotechnol.*, 2006, **124**, 670-689.
21. M. M. E. Huijbers, S. Montersino, A. H. Westphal, D. Tischler and W. J. H. van Berkel, *Arc. Biochem. Biophys.*, 2014, **544**, 2-17.
22. K. Crozier-Reabe and G. R. Moran, *Int. J. Mol. Sci.*, 2012, **13**, 15601-15639.